HHS Public Access

Author manuscript

Exp Neurol. Author manuscript; available in PMC 2021 April 05.

Published in final edited form as:

Exp Neurol. 2020 March ; 325: 113120. doi:10.1016/j.expneurol.2019.113120.

FTY720-Mitoxy Reduces Synucleinopathy and Neuroinflammation, Restores Behavior and Mitochondria Function, and Increases GDNF Expression In Multiple System Atrophy Mice

Guadalupe Vidal-Martinez[a], **Ismael Segura-Ulate**[a], **Barbara Yang**[a], **Valeria Diaz-Pacheco**[a], **Jose A. Barragan**[a], **Jocelyn De-Leon Esquivel**[a], **Stephanie A. Chaparro**[a], **Javier Vargas-Medrano**[a], **Ruth G. Perez**[a,#]

[a]Texas Tech University Health Sciences Center El Paso, Department of Molecular and Translational Medicine, Center of Emphasis in Neurosciences, Graduate School of Biomedical Sciences, Paul L Foster School of Medicine, 5001 El Paso Dr, El Paso, TX 79905.

Abstract

Multiple system atrophy (MSA) is a fatal disorder with no effective treatment. MSA pathology is characterized by α-synuclein (aSyn) accumulation in oligodendrocytes, the myelinating glial cells of the central nervous system (CNS). aSyn accumulation in oligodendrocytes forms the pathognomonic glial cytoplasmic inclusions (GCIs) of MSA. MSA aSyn pathology is also associated with motor and autonomic dysfunction, including an impaired ability to sweat. MSA patients have abnormal CNS expression of glial-cell-line-derived neurotrophic factor (GDNF) and brain-derived neurotrophic factor (BDNF). Our prior studies using the parent compound FTY720, a food and drug administration (FDA) approved immunosuppressive for multiple sclerosis, reveal that FTY720 protects parkinsonian mice by increasing BDNF. Our FTY720-derivative, FTY720-Mitoxy, is known to increase expression of oligodendrocyte BDNF, GDNF, and nerve growth factor (NGF) but does not reduce levels of circulating lymphocytes as it is not phosphorylated so cannot modulate sphingosine 1 phosphate receptors (S1PRs), so it is not immunosuppressive. To preclinically assess FTY720-Mitoxy for MSA, we used mice expressing human aSyn in oligodendrocytes under a 2,' 3'-cyclic nucleotide 3'-phosphodiesterase (CNP) promoter. CNP-aSyn transgenic (Tg) mice develop motor dysfunction between 7 – 9 mo, and progressive GCI pathology. Using liquid chromatography-mass spectrometry (LC-MS/MS) and enzymatic assays, we confirmed that FTY720-Mitoxy was stable and active. Vehicle or FTY720-Mitoxy (1.1 mg/kg/day) was delivered to wild type (WT) or Tg littermates from 8.5 – 11.5 mo by osmotic pump. We

[#]To whom correspondence should be addressed. Current affiliation and contact information: R & R Perez LLC, 6005 Alcalde St., El Paso, TX 79912, Phone: 724-493-4460, rperezllc@gmail.com.

Current address for Dr. Segura-Ulate: Institute of Pharmacological Investigations, University of Costa Rica, San Jose, CR.

Conflict of interest statement:

Corresponding author holds US patent # 10391066, "Compositions and Methods for the Treatment of Parkinson's isease", also filed in Canada (CA 2888634) and Mexico (MX 004806), which does not alter adherence to Experimental Neurology policies.

behaviorally assessed their movement by rotarod and sweat production by starch-iodine test. Postmortem tissues were evaluated by qPCR for BDNF, GDNF, NGF and GDNF-receptor RET mRNA and for aSyn, BDNF, GDNF, and Iba1 protein by immunoblot. MicroRNAs (miRNAs) were also assessed by qPCR. FTY720-Mitoxy normalized movement, sweat function and soleus muscle mass in 11.5 mo Tg MSA mice. FTY720-Mitoxy also increased levels of brain GDNF and reduced brain miR-96–5p, a miRNA that acts to decrease GDNF expression. Moreover, FTY720-Mitoxy blocked aSyn pathology measured by sequential protein extraction and immunoblot, and microglial activation assessed by immunohistochemistry and immunoblot. In the 3-nitropropionic acid (3NP) toxin model of MSA, FTY720-Mitoxy protected movement and mitochondria in WT and CNP-aSyn Tg littermates. Our data confirm potent *in vivo* protection by FTY720-Mitoxy, supporting its further evaluation as a potential therapy for MSA and related synucleinopathies.

1. Introduction

Among the most aggressive and debilitating of all age-related movement disorders is the orphan disease called multiple system atrophy (MSA). MSA patients suffer parkinsonian, cerebellar, pyramidal, and autonomic symptoms (Fanciulli and Wenning, 2015; Jellinger, 2016; Stefanova and Wenning, 2016; Ubhi et al., 2011). MSA pathology is associated with aSyn accumulation in the myelinating oligodendrocytes of the CNS (Ahmed et al., 2013; Fanciulli and Wenning, 2015; Papp et al., 1989; Stefanova and Wenning, 2016). MSA-aSyn-aggregates in GCIs are linked to oligodendrocyte loss and demyelination (Dickson et al., 1999; Jellinger, 2014; Miller et al., 2004; Ubhi et al., 2011; Wakabayashi et al., 1998). Symptoms similar to Parkinson's disease define parkinsonian type MSA (MSA-P), which manifests with rigidity, paralysis, and postural instability as well as striatonigral degeneration (SND). The cerebellar subtype called MSA-C primarily shows olivopontocerebellar atrophy (OPCA) and cerebellar ataxia. Both types of MSA exhibit cerebellar pathology (Ishizawa et al., 2004). Autonomic problems are also common in all forms of MSA and include impaired sweating, as well as cardiovascular, sexual, urogenital, and gastrointestinal dysfunction (Coon et al., 2017; Jecmenica-Lukic et al., 2012; Jellinger, 2014; Jellinger et al., 2005; Kihara et al., 1991; Ubhi et al., 2011; Verstappen and Bloem, 2007). Moreover, the myelinating glia of the peripheral nervous system, the Schwann cells (SC), contain aSyn cytoplasmic inclusions called SCCIs in cranial and spinal nerves, peripheral ganglia and the visceral autonomic innervation of MSA (Nakamura et al., 2015). Thus, therapies that improve not only movement but also autonomic function could be particularly beneficial for improving the quality of life for MSA patients.

With regard to BDNF and GDNF in MSA, both have abnormal expression in the dendrites of cerebellar Purkinje cells as measured by immunostaining (Kawamoto et al., 1999; Kawamoto et al., 2000). Furthermore, data from our laboratory and others confirm that BDNF becomes downregulated in oligodendrocytes when aSyn accumulates (May et al., 2014; Segura-Ulate et al., 2017b). A reduction in BDNF and GDNF also occurs in mice that overexpress aSyn under a myelin basic protein (MBP) promoter, the MBP-aSyn MSA mice (Ubhi et al., 2012; Ubhi et al., 2010). GDNF delivery improves MBP-aSyn mouse movement (Ubhi et al., 2010), as does fluoxetine, a drug that increases both BDNF and GDNF and reduces MSA-like motor impairment in MBP-aSyn mice (Ubhi et al., 2012). Yet,

MBP-aSyn mice undergo almost no SND, suggesting that their motor loss may be associated with brainstem, spinal cord, or cerebellar impairment. Another MSA model, mice that expresses aSyn in oligodendrocytes under the proteolipid protein (PLP) promoter (PLP-aSyn mice) (Kahle et al., 2002) show SND that is common to MSA-P. Both MBP-aSyn and PLP-aSyn mice model the progressive motor and autonomic dysfunction seen in MSA (Stefanova and Wenning, 2015). Also, PLP-aSyn mice show microglial activation and brain GCI-like aSyn pathology (Stefanova et al., 2007), as well as BDNF and GDNF changes that vary with age and CNS region (Refolo et al., 2018). A third MSA model, the CNP-aSyn mice, though not as extensively studied as the MBP-aSyn and PLP-aSyn mice, also develops progressive motor and autonomic dysfunction as well as neuropil and white matter damage associated with aSyn pathology (Giasson et al., 2003; Yazawa et al., 2005), as occurs in MSA-P and MSA-C patients (Minnerop et al., 2010). Thus, though MSA models are imperfect, they still have predictive value for therapy development (Overk et al., 2018). We obtained CNP-aSyn MSA mice in which to measure behavior, pathology, trophic factor expression, microglial activation, and responses to 3NP ± a FTY720-Mitoxy, measures not previously assessed in this model.

We have studied *in vitro* and *in vivo* effects of the parent compound FTY720 (fingolimod, Gilenya), an approved multiple sclerosis drug, on trophic factor expression. We and others show that FTY720 increases BDNF in cell and animal models (Deogracias et al., 2012; Di Pardo et al., 2014; Doi et al., 2013; Fukumoto et al., 2014; Hait et al., 2014; Heinen et al., 2015; Noda et al., 2013; Schuhmann et al., 2016; Segura-Ulate et al., 2017b; Vargas-Medrano et al., 2014; Vidal-Martinez et al., 2016). FTY720 also increases GDNF expression in astrocytes and microglia (Janssen et al., 2015; Noda et al., 2013). However, FTY720 induces immunosuppression by interacting with S1PRs to reduce circulating blood T cells (Ayzenberg et al., 2016; Chiba et al., 1998; Morris et al., 2005; Paugh et al., 2003). As our derivative, FTY720-Mitoxy is not phosphorylated; it cannot modulate S1P receptors or alter T cell levels thus, our patented derivative is not immunosuppressive (Enoru et al., 2016; Segura-Ulate et al., 2017a; Segura-Ulate et al., 2017b; Vargas-Medrano et al., 2019). While multiple sclerosis patients benefit from such immunosuppression and FTY720 might be repurposed to treat MSA, immunosuppression could be problematic when treating an aging disorder.

In addition to movement and autonomic dysfunction in MSA, is a finding of mitochondrial abnormalities. For instance, MSA skeletal muscle shows mitochondrial dysregulation (Blin et al., 1994) and there are losses in mitochondrial complex II and III activity in stem-cell-derived-dopaminergic-neurons from MSA patients (Alsemari and Al-Hindi, 2015; Monzio Compagnoni et al., 2018). Also, MBP-aSyn mice show mitochondrial abnormalities in oligodendrocytes that are linked with aSyn aggregation (Overk et al., 2018; Shults et al., 2005). Notably, MSA models can also be generated using mitochondrial toxins. For example, 1-methyl-4-phenyl-1, 2, 3, 6-tetrahydropyridine (MPTP) + 3NP induces MSA-like nigrostriatal and striatopallidal damage in 2 mo old WT mice (Stefanova et al., 2003). In other models, symptomatic MBP-aSyn mice treated with 3NP have more severe motor loss and MSA-like-aSyn nitration/oxidation, while PLP-aSyn mice have increased microglial activation in cerebellar white matter (Stefanova et al., 2005; Ubhi et al., 2009). With this in mind, we hypothesized that a therapy that can protect mitochondria and reduce microglial

activation, as also occurs in MSA-P and MSA-C (Ishizawa et al., 2004), may be especially beneficial for those with MSA. We created FTY720-Mitoxy by adding a triphenylphosphonium (TPP) moiety to the parent compound FTY720, to localize the derivative to presynaptic sites that are enriched in mitochondria (Chinnasamy et al., 2010; Vargas-Medrano et al., 2014; Zielonka et al., 2017).

Over time we have confirmed that FTY720-Mitoxy rapidly crosses the blood brain barrier, increases neuronal BDNF expression, increases oligodendroglial GDNF, BDNF, and NGF expression and does not immunosuppress by reducing circulating T cells (Enoru et al., 2016; Segura-Ulate et al., 2017a; Vargas-Medrano et al., 2014; Vargas-Medrano et al., 2019). As innervation of eccrine sweat gland utilizes GDNF, NGF as well as acetylcholine (Christianson et al., 2003; Grant et al., 1995; Landis et al., 1985; Yoshida, 2004), we hypothesized that FTY720-Mitoxy's ability to increase trophic factor expression would improve sweat function (Vargas-Medrano et al., 2014; Vargas-Medrano et al., 2019).

We tested FTY720-Mitoxy on MSA-like impairments in CNP-aSyn Tg mice that develop motor loss between 7 – 9 mo (Yazawa et al., 2005), similar to MBP-aSyn mice (6 mo), and earlier than PLP-aSyn mice (12 mo). We treated CNP-aSyn mice with FTY720-Mitoxy from 8.5 mo, and saw improved behavior. In addition, FTY720-Mitoxy reduced spinal cord aSyn aggregation and cerebellar white matter microglial activation. This occurred in parallel with frontal cortex/corpus callosum GDNF increase at both protein and mRNA levels and reduced expression of miR-96–5p, a microRNA that acts to downregulate GDNF (Alberico et al., 2015). By modeling MSA in mice using 3NP, our studies revealed that, FTY720-Mitoxy reduced MSA-like-impairments in both WT and CNP-aSyn Tg mice by counteracting loss of succinate dehydrogenase (SDH; EC 1.5.3.1), mitochondrial Complex II activity. Cumulatively, these preclinical data support further testing of FTY720-Mitoxy as a candidate therapy for MSA and related synucleinopathies.

2. Materials and methods

2.1.1. Animals—CNP-aSyn (B6:C3-Tg-CNP-SNCA-M2Vle) breeders were generously provided by Dr. Virginia Lee (University of Pennsylvania, Philadelphia, PA) (Giasson et al., 2003; Yazawa et al., 2005) from a repository at the Jackson Laboratories (Bar Harbor, ME). Non-littermate heterozygous CNP-aSyn breeders (N = 6, 4 females, 2 males) were used to generate our cohort of male and female Tg and WT littermates for our studies. Heterozygous and homozygous Tg mice express one or two copies of WT human *SNCA*, respectively, driven by the CNP promoter to express aSyn in myelinating oligodendrocytes of CNS and peripheral nervous system (PNS) Schwann cells (Giasson et al., 2003; Yazawa et al., 2005). Mice were housed (2 – 5 per group) in barrier cages on ventilated racks in pathogen free rooms with temperature and humidity-control on 12 hr light/dark cycles. Food and water were available *ad libitum*. Ethical treatment of animals followed AALAC, ARRIVE, and NIH guidelines on Texas Tech University Health Sciences Center Institutional Animal Care and Use Committee (IACUC) approved breeding and experimental protocols. CNP-aSyn Tg mice and WT littermates were randomly assigned to groups (Research Randomizer, https://www.randomizer.org) with mice and data assessed by experimenters blinded to the conditions.

2.1.2. Genotyping—Using the protocol kindly provided by Ms. Susan Leight of Dr. Virginia Lee's laboratory, genomic DNA from pups was used to measure human *SNCA* copy number by real time quantitative PCR (qPCR) with the following primers SNCA Fwd: 5'-GGAGCAGGGAGCATTGCA-3' and SNCA Rev: 5'-CCTTCTTCATTCTTGCCCAACT-3'. Murine *Gapdh* gene was used as an endogenous control, with levels detected by the following primers Gapdh Fwd: 5'-CCTGCTCCCCCTACACACA-3' and Gapdh Rev: 5'-CCTGTTCTTCTCGGGCAAAA-3', with qPCR performed using the RealPlex Mastercycler 2 (Eppendorf, Hauppauge, NY) and GoTaq qPCR Master Mix (Cat # A6001, Promega, Madison, WI). Thermal qPCR conditions were: pre-PCR hold for 1 min at 60°C, pre-PCR hold for 10 min at 95°C, followed by 40 cycles of 15 sec each at 95°C then 1 min at 60°C followed by fluorescence emission detection. Levels of human *SNCA* and murine *Gapdh* were quantified and compared to one of the heterozygous Tg CNP-aSyn breeders originally provided by Jackson Laboratories. Relative fold changes of human SNCA were determined by the comparative cycle threshold method ($2^{-\Delta\Delta}$Ct) and interpreted as follows: 0 = WT, 1 = Tg heterozygous CNP-aSyn and ≥2 = Tg homozygous CNP-aSyn.

2.2. FTY720-Mitoxy is stable and accumulates in mitochondria

Liquid chromatography (LC) separates compounds on a column, and then spectrometry (MS) is used to measures the mass of the compound, which for FTY720-Mitoxy produced a single peak, confirming that no breakdown of the compound occurred (Enoru et al., 2016). LC/MS/MS assessed FTY720-Mitoxy stability for a sample that was aged 3 yr at −20°C and compared to freshly prepared FTY720-Mitoxy in solution. Both had single peaks (Fig. 1b, top and middle chromatograms), confirming long term stability of the drug. To test FTY720-Mitoxy stability at body temperature, drug was prepared in lactated Ringer's solution then incubated at 37°C in sterile O-ring tubes for 42 days (the lifetime of Alzet Model 2006 pump). Tubes were spun to collect full samples for physiological evaluation of FTY720-Mitoxy effects on PP2A enzymatic activity in MN9D cells (Vargas-Medrano et al., 2014). Briefly, cells were treated 30 min with Vehicle, 5 μM of FTY720, fresh FTY720-Mitoxy, or the 42 day aged FTY720-Mitoxy. Cells were prepared as before (Peng et al., 2005) with protein concentration determined by bicinchoninic acid (BCA) assay (Smith et al., 1985). Using 150 μg of cell lysate per sample, PP2A catalytic subunit (PP2Ac) was immunoprecipitated from lysates using anti-PP2Ac antibody 1D6 (Cat # 05–421, EMD Millipore, Burlington, MA, USA) + protein A beads (Cat # 20333, ThermoFisher Scientific, Waltham, MA, USA). Activity of immunoprecipitated PP2Ac was then measured relative to freshly prepared standards using the malachite green assay as before (Lek et al., 2017; Vargas-Medrano et al., 2014) with samples read at 630 nm (Multiskan Spectrum, ThermoFisher Scientific) (Fig. 1c).

FTY720-Mitoxy, though not orally bioavailable, rapidly crosses the blood brain barrier (Enoru et al., 2016) and protects both neuronal and oligodendrocyte cells (Segura-Ulate et al., 2017b; Vargas-Medrano et al., 2014; Vargas-Medrano et al., 2019; Vargas-Medrano et al., 2018). Briefly, MN9D cells were treated 30 min with 5 μM FTY720-Mitoxy, a dose that is within a linear range for stimulating PP2A activity when compared to aSyn in dose response experiments (see Figs. 1 and 4 of Vargas-Medrano et al, 2014 for details).

Mitochondria were isolated using a kit (Cat# 89874, ThermoFisher Scientific) and validated to be mitochondria as those samples contained heat shock protein 60 (HSP60) and cyclooxygenase 4 (COX4) that were not present in cytosol of MN9D cells (not shown). LC/MS/MS of MN9D mitochondria was performed by Ricerca Biosciences LLC (now Concord Biosciences LLC, a Frontage Company, Concord, OH, USA) which confirmed that intact FTY720-Mitoxy was present in mitochondria (Fig. 1b, bottom chromatogram).

2.3 Subcutaneous drug delivery by osmotic pump

FTY720-Mitoxy synthesis and pharmacokinetics have been described (Enoru et al., 2016; Vargas-Medrano et al., 2014). Intravenously delivered FTY720-Mitoxy enters brain in 5 min and is present in brain for at least 48 hr (Enoru et al., 2016). A stock solution of 150 mM FTY720-Mitoxy was prepared in 200 proof ethanol, then dissolved in Ringer's lactate solution (Cat # sc-516304 Rx, Santa Cruz Animal Health, Santa Cruz, CA, USA). Mice received FTY720-Mitoxy (1.1 mg/kg/day) by continuous release using Model 2006 pumps from Alzet Corporation (Cupertino, CA, USA) for 84 days. Pumps containing FTY720-Mitoxy or Vehicle were subcutaneously implanted through an incision between the scapulae of WT or CNP-aSyn Tg mice (8.5 mo, ≥ 20 gm weight) under general anesthesia. During recovery, pumps move from a dorsomedial to a lateral position on the animal's back, which still allows normal movement for behavioral tests. The pump life of Model 2006 is 42 days, so after 42 days, a second pump was implanted to deliver drug to 11.5 mo according to the time line shown (Fig. 1d). In separate experiments to assess the impact of FTY720-Mitoxy on mitochondria *in vivo*, we used Alzet pumps (Model 2002) to deliver FTY720-Mitoxy for 14 days with Vehicle or 3NP given as described below.

2.4 Behavioral analysis

Behavioral tests were performed at 6 mo, 8 mo, 10 mo and 11.5 mo. Experiments were conducted in clean quiet test rooms at Texas Tech University Health Science Center Laboratory Animal Resources Center (LARC). Animals were transferred to test rooms at least 15 min before to allow them to acclimate to the novel environment prior to testing.

2.4.1. Movement—Balance and coordination were measured by rotarod (Cat # LE8200, Harvard Apparatus, Holliston, MA), which also measures endurance in N = 138 mice, (WT = 68, Tg = 70). Rotarod timing as "latency to fall" from the apparatus was recorded in sec using established methods (Giasson et al., 2002; Graham and Sidhu, 2010). Briefly, mice were familiarized with the rotarod during initial trainings of 2 sessions on 2 consecutive days. Each training session consisted of 2 runs lasting 2 min each, one at 4 revolutions per min (rpm) and the other at 8 rpm. Experimental data were collected in 3 runs/day on 2 different days for each mouse, with rotation increasing from 4–40 rpm over 5 min time. A minimum 5 min rest period was allowed between runs for all mice.

2.4.2. Sweat analysis—As a measure of autonomic injury consistent with MSA, sweat droplets were measured by the method of Liu, et al. (2017) with minor modifications in N = 41 mice, (WT = 19, Tg = 32). Briefly, mice were gently and firmly manually restrained by one experimenter throughout each test. Another experimenter cleaned the left hind paw with a water-moistened cotton tipped swab. Then the second experimenter painted the hind paw

using a small artist brush dipped in a freshly prepared solution of 2% iodine (Cat # 207772, Sigma-Aldrich, St. Louis, MO, USA) prepared in ethanol. After the paw had dried, it was then painted with a starch solution prepared in castor oil (1g/mL, Cat # S9765 in Cat # 259853, Sigma-Aldrich, St. Louis, MO, USA). The paw was then photographed through a 10X magnifier lens at 0, 2.5 and 5 min to record dark purple precipitates that formed. Digital images were then blind coded and analyzed using ImageQuant 5.2 software (GE Healthcare, Waukesha, WI) to quantify sweat droplets in arbitrary units on the main area of the paw (outlined areas shown in Fig. 4a) overlying the eccrine sweat glands. Sweat drops on the digits were not included in the quantification.

2.5. Evaluation of mitochondrial toxin 3NP ± FTY720-Mitoxy in WT and Tg mice

Osmotic pumps with FTY720-Mitoxy in Ringer's lactate delivered 1.1 mg/kg/day to 8.5 mo old WT or CNP-aSyn Tg mice from day 0 to 14 (time span of Alzet model 2002 pump) in N = 24 mice, (WT = 8, Tg = 16). The 3NP toxin (Cat # N5634, Sigma-Aldrich, St. Louis, MO, USA), an inhibitor of mitochondrial SDH, also known as mitochondrial Complex II (Scallet et al., 2001), was prepared in sterile saline (pH 7.4). Vehicle consisted of an equal volume of sterile saline. On day 9.5, mice received twice daily subcutaneous injections of 3NP using methods previously used in MSA mice (Ubhi et al., 2009) as follows: 10 mg/kg (day 9.5), 20 mg/kg (days 11 and 12), and 30 mg/kg (days 13 and 14) or Vehicle control solution.

2.6. Tissue collection and handling

Mice were euthanized by CO_2 inhalation followed by decapitation. Tissues for protein and/or RNA were rapidly collected and included brain, spinal cord, paw sweat pads, and soleus muscles. Most tissues were frozen on dry ice then stored at −80°C until use. For total RNA, fresh tissues were submerged in RNA-later solution (Cat # AM7020, ThermoFisher Scientific) then incubated at 4°C overnight prior to transfer to −20°C for storage, as per manufacturer. Some RNA extractions were performed using tissues stored at −80°C, to which we added RNA-later-ICE (Cat # AM7030, ThermoFisher Scientific) followed by overnight incubation at −20°C before subsequent processing.

2.7. Gene and microRNA expression

2.7.1. Gene expression—Total mRNAs were extracted from brain and paw sweat glands using the RNeasy Plus Mini Kit (Cat # 74134, Qiagen Inc., Valencia, CA) then retrotranscribed using a High Capacity RNA-to-cDNA Kit (Cat # 4387406, ThermoFisher Scientific), as per manufacturer. Total miRNAs from brain were extracted using the miRNeasy Mini Kit (Cat # 217004, Qiagen) according to the manufacturer. Retrotranscription of mature miRNAs was performed using the miScript II RT Kit (Cat # 218160, Qiagen). RNA concentration and purity were confirmed using NanoDrop 2000 spectrophotometry (ThermoFisher Scientific). Integrity of RNAs and assessment for genomic DNA contamination were done by evaluating 28S/18S rRNAs band ratios on RNA "bleach" gels as before (Aranda et al., 2012; Segura-Ulate et al., 2017b; Vargas-Medrano et al., 2018). The mRNA and miRNA levels were measured by qPCR using the RealPlex Mastercycler 2 described above. Relative expression of mRNAs was evaluated using Taqman assays (ThermoFisher Scientific) for mouse BDNF (Cat # Mm04230607_s1),

mouse NGF (Cat # Mm00443039_m1), mouse RET (Cat # Mm00436304_m1), and mouse GDNF (Cat # Mm00599849_m1), with mouse Gapdh (Cat # Mm99999915_g1) as an internal control. Reactions were carried out in triplicate using GoTaq Probe qPCR Master Mix (Promega, Cat # A6102).

2.7.2. MicroRNA expression—Relative expression of miR-96–5p was determined using miScript primer assays (Qiagen) for mature mm-miR-96–5p (Cat # MS00001456). Internal expression controls were performed with miScript primer assays for SNORD72 (Cat # MS00033719) and SNORD95 (Cat # MS00033726) and miScript miRTC (Cat # MS00000001) primer assay. Reactions were carried out in triplicate using the miScript Sybr Green qPCR Kit (Cat # 218075, Qiagen).

2.8.1. Mitochondria isolation—Brain mitochondria were isolated using a kit (Cat # 89801, ThermoFisher Scientific) according to the manufacturer. Protease inhibitors that were added to all solutions included 17 ug/mL aprotinin, 1 mM benzamidine, and 1 mM AEBSF. Dounce homogenization of 200 mg cerebellum/mouse was performed on ice to isolate mitochondria. The mitochondrial fraction was purified by centrifugation steps in which a final pellet containing mitochondria was suspended in 50 μl sterile PBS. Total protein concentration of isolated mitochondria was determined by BCA analysis described above.

2.8.2. Succinate dehydrogenase assay of isolated mitochondria—SDH activity was measured using 60 μg of purified mitochondrial protein for all conditions using a colorimetric assay (Cat # MAK197–1KT, Sigma-Aldrich, St. Louis, MO USA). Briefly, mitochondria were added to the reaction mixture in a 96-well plate. Initial absorbance was measured at 600 nm at baseline (time 0), then again after 30 min incubation at 25°C. SDH activity was determined relative to freshly prepared standards read at 600 nm in a plate reader (Multiskan Spectrum, ThermoFisher Scientific). The difference between the two readings was used to calculate SDH activity as defined in the kit protocol.

2.9. Protein assessments

2.9.1. Immunoblots—Protein concentrations were determined by BCA assay as described above. Proteins (25–50 μg per lane) were separated by SDS-PAGE, transferred to nitrocellulose, stained with Ponceau S to assess transfer, blocked with 5% non-fat dry milk in buffer 1 hr at room temperature, and incubated at 4°C in primary antibody overnight. For dot blots, equal protein amounts were applied to nitrocellulose with blots handled as described above. Blots were imaged using LiCor Odyssey (Model 9210, LiCor Biosciences, Lincoln, NE, USA) and quantified with LiCor Image Studio software or ImageQuant software (GE Healthcare Technologies, Waukesha, WI, USA).

2.9.2. Antibodies—Antibodies included: total aSyn (Cat # sc-7011-R, Santa Cruz Biotechnology Inc., 1:200), PSer129 aSyn (Cat# SAB4503996, Millipore Sigma, St. Louis, MO, 1:100), GDNF (Cat # ab18956, Abcam, Cambridge, MA, 1:500), Iba1 (Cat# 016–20001, FujiFilm/Wako Pure Chemical Corp., Richmond, VA, USA; 1:200) and β-actin (Cat # 3700 or 4970 Cell Signaling Technology Inc., 1:1000). Infrared signals were produced

using anti-mouse, anti-goat, or anti-rabbit secondary antibodies coupled to IgG IRDye680 or IgG IRDye800 (Rockland Immunochemicals, Gilbertsville, PA, USA, 1:5000 – 1:10,000).

2.9.3. Sequential protein extractions—Please note that this method does not isolate cellular and subcellular fractions, but rather separates soluble from insoluble proteins in a series of buffers using ultracentrifugation for pellet re-extractions. Thus loading controls are unavailable when using this method. Protein extraction from lumbar spinal cord was performed according to Waxman and Giasson (2008) as detailed in Wu et al. (2012) and Vidal-Martinez et al. (Vidal-Martinez et al., 2016). Soluble and insoluble proteins were isolated using a series of 4 buffers with pellets re-extracted after ultracentrifugation for 30 min at 100,000 × g (4°C). Extraction buffers were: (1) high-salt (**HS**) containing 50 mM Tris-HCl (pH 8.0), 750 mM NaCl, and 5 mM EDTA; (2) high salt Triton X-100 (**HST**) containing 50 mM Tris-HCl (pH 8.0), 750 mM NaCl, 5 mM EDTA, (3) 1% Triton X-100; radioimmunoprecipitation assay buffer (**RIPA**) containing 50 mM Tris-HCl (pH 8.0), 150 mM NaCl, 5 mM EDTA, 1% NP-40, 0.5% Sodium deoxycholate, and (4) 0.1% SDS; Sodium dodecylsulfate + Urea (**SDS/Urea**) containing 10 mM Tris-HCl (pH 7.5), 8 M Urea, 2% SDS. Protease inhibitors included 17 μg/mL aprotinin, 1 mM benzamidine, and 1 mM AEBSF in all buffers.

2.10. Statistical analyses

Data represent mean ± standard deviation (SD) of 3 or more independent experiments. Unpaired two-tailed Student's t-tests, One way ANOVA, or Two way repeated measures ANOVA were performed using Prism 8 (GraphPad Software Inc., La Jolla, CA) with significance set to $p < .05$. Linear regression was performed using GraphPad QuickCalcs. Relative mRNA or miRNA expression was calculated by the $2^{-\Delta\Delta Ct}$ method using Relative Expression Software Tool (REST-2009, Qiagen) (Pfaffl et al., 2002). Whisker box plots generated with REST-2009, show relative mRNA or miRNA expression as median (dashed midline inside the box), interquartile ranges 1 and 3 (upper and lower edges of the box), and maximum and minimum expression values (top and bottom whiskers) (Pfaffl et al., 2002). We are aware of growing concerns about the indiscriminate use of p values as the sole measure of statistical significance (Wasserstein et al., 2019). Thus, we discuss why the differences found appear to be meaningful.

3. Results

3.1. FTY720-Mitoxy is stable in solution

Chemical structures of FTY720 and the FTY720-Mitoxy derivative are shown in Figure 1a. FTY720 parent compound is stable in solution (Morris et al., 2005), but we needed to ascertain if FTY720-Mitoxy was stable in solution and was present in mitochondria. To assess this we performed LC-MS/MS of fresh 1 μM FTY720-Mitoxy in solution (Fig. 1b, top chromatogram), 1 μM FTY720-Mitoxy in solution stored 3 yr at −20°C (Fig. 1b, middle chromatogram), and FTY720-Mitoxy in mitochondria purified from cells (Fig. 1b, bottom chromatogram). All LC-MS/MS chromatograms had single peaks with identical retention times, confirming FTY720-Mitoxy stability in solution as well as in mitochondria. To test if FTY720-Mitoxy is stable at body temperature (Fig.1c), we incubated FTY720-Mitoxy

solution at 37°C for 42 days (the lifetime of Alzet pump Model 2006) then measured its ability to physiologically stimulate PP2A activity in cultured cells in 3 independent experiments using well-established methods (Lek et al., 2017; Vargas-Medrano et al., 2014). Briefly, we treated MN9D cells with 5 μM of FTY720 (N = 3), FTY720-Mitoxy (N = 3), or 5 μM FTY720-Mitoxy aged 42 day at 37°C (N = 3). All FTY720s stimulated endogenous PP2A activity above Vehicle levels, showing meaningful differences and confirming the stability of the drug at body temperature (Two way repeated measures (RM) ANOVA, $p = .009$). Tukey multiple comparisons show significant differences compared to Vehicle for fresh FTY720 ($p = .0064$), fresh FTY720-Mitoxy ($p = .0114$), or FTY720-Mitoxy 42 day aged at 37°C ($p = .0065$), verifying that physiologically active FTY720-Mitoxy could be delivered by osmotic pump using the timeline shown (Fig. 1d).

3.2. FTY720-Mitoxy counteracts motor deficits in aging CNP-aSyn Tg mice

Impaired motor function is seen in all MSA mice that express human aSyn in oligodendrocytes (Shults et al., 2005; Stefanova et al., 2005; Yazawa et al., 2005). Measuring motor behavior by rotarod is an established method used to define both MSA-like onset and progression (Kuzdas-Wood et al., 2015; Shults et al., 2005; Yazawa et al., 2005). In CNP-aSyn mice at 6 mo, we saw that rotarod performance was similar for both WT and CNP-aSyn Tg littermates (not shown) as previously confirmed (Yazawa et al., 2005). By 8 mo, CNP-aSyn Tg mice had impaired rotarod performance compared to WT littermates (Fig. 2a). Thus, we began delivering Vehicle or FTY720-Mitoxy by osmotic pump when mice were 8.5 mo old. It is noteworthy that CNP-aSyn Tg MSA mice that are untreated perform similarly on rotarod between 7 – 12 mo (Yazawa et al., 2005). We saw movement differences between treatment groups at 10 mo (One way ANOVA, Fig. 2b, $p = .00009$) and 11.5 mo (One way ANOVA, Fig. 2c, $p = .00009$). Tukey multiple comparisons showed that WT mice (N = 68) did similarly on rotarod at 10 mo when treated with Vehicle (Fig. 2b) ($\overline{X} \pm SD = 90.44 \pm 35.28$ at 10 mo); or at 11.5 mo when treated with Vehicle (Fig. 2c) ($\overline{X} \pm SD = 87.8 \pm 41.8$ at 11.5 mo) or when treated with FTY720-Mitoxy (Fig. 2b, 10 mo) ($\overline{X} \pm SD = 93.97 \pm 37.5$ at 10 mo, $p = .61$, ns); or (Fig. 2c, 11.5 mo) ($\overline{X} \pm SD = 91.6 \pm 32.6$ at 11.5 mo, $p = .91$, ns). In contrast, Vehicle treated CNP-aSyn Tg mice (N = 70) had poorer rotarod performance than Vehicle treated WT littermates (Fig. 2b, 10 mo) ($\overline{X} \pm SD = 79.37 \pm 34.41$, $p = .014$); or (Fig. 2c, 11.5 mo) ($\overline{X} \pm SD = 76.4 \pm 40.2$, $p = .039$). After FTY720-Mitoxy, 10 mo and 11.5 mo CNP-aSyn Tg mice did significantly better than Vehicle treated Tg littermates (Fig. 2b, 10 mo) ($\overline{X} \pm SD = 99.22 \pm 38.51$, $p = .00009$); (Fig. 2c, 11.5 mo) ($\overline{X} \pm SD = 101.5 \pm 45.9$ at 11.5 mo, $p = .00009$) suggesting that motor deficits were reversed by FTY720-Mitoxy.

3.3. FTY720-Mitoxy contributes to increased soleus muscle weight in CNP-aSyn Tg mice

Muscle wasting occurs in MSA (Rehman, 2001). It has also been shown that mouse soleus muscle mass increases in parallel with rotarod performance (Yu et al., 2018) and that soleus muscles exhibit an oxidative metabolic phenotype with increased mitochondrial content (Crupi et al., 2018). To further explore FTY720-Mitoxy effects in CNP-aSyn mice, we weighed soleus muscles of WT (N = 14) and Tg (N = 32) mice and discovered meaningful differences (Fig. 3, One way ANOVA $p = .046$). Overall, soleus muscle weights were similar

in WT Vehicle ($\overline{X} \pm SD = 9.9 \pm 1.7$), WT FTY720-Mitoxy ($\overline{X} \pm SD = 10.2 \pm 2.1$), and Tg FTY720-Mitoxy treated mice ($\overline{X} \pm SD = 10.9 \pm 2.6$), though sizes overlap in all conditions. However, the MSA-like Vehicle treated CNP-aSyn Tg mice had significantly smaller soleus muscles than all others, as assessed by Tukey multiple comparisons ($\overline{X} \pm SD = 8.7 \pm 1.2$, $p = .02$). Smaller muscles in Tg Vehicle treated mice related to their poorer rotarod performance, while increased soleus muscle mass in FTY720-Mitoxy treated Tg mice also related to their longer rotarod times (Fig. 2).

3.4. FTY720-Mitoxy enhances sweat function and RET mRNA in CNP-aSyn Tg hind paw

MSA patients suffer from hypohidrosis or anhidrosis, a reduction or loss of the ability to sweat, especially in their lower extremities (Coon et al., 2017; Kihara et al., 1991; Lipp et al., 2009; Verstappen and Bloem, 2007). However, the effect of a therapeutic on sweat production has never been tested in MSA mice. We measured hind paw sweat droplet signal by iodinestarch test with densitometry measured in arbitrary units (as detailed in Materials and methods) (Fig. 4a) in Vehicle or FTY720-Mitoxy treated WT and Tg mice. We tested WT (N = 19) and CNP-aSyn Tg littermates (N = 32) and found meaningful differences in their ability to sweat (Fig. 4b, One way ANOVA, $p = .0026$). Tukey multiple comparisons showed that WT mice had similar sweat signal when treated with Vehicle ($\overline{X} \pm SD = 13668 \pm 2891$) or FTY720-Mitoxy ($\overline{X} \pm SD = 15827 \pm 3967$, $p = .78$). In contrast, Vehicle treated CNP aSyn Tg MSA mice had significantly lower sweat signal ($\overline{X} \pm SD = 9281 \pm 4005$) compared to FTY720-Mitoxy treated Tg littermates ($\overline{X} \pm SD = 15530 \pm 6795$, $p = .0041$), that had sweat signal much more similar to FTY720-Mitoxy treated WT littermates ($\text{Tg Mitoxy } \overline{X} \pm SD = 15530 \pm 6795$, $\text{WT Mitoxy } \overline{X} \pm SD = 15827 \pm 3967$, $p = .99$).

We next assessed trophic factor-related mRNAs to ascertain if FTY720-Mitoxy may have improved sweating in such a manner. We measured mRNA levels of GDNF, NGF, and RET (a GDNF receptor) in the sweat pads of representative WT (N = 8) and CNP aSyn Tg (N = 8) mice, as these factors contribute to sweat gland innervation. There was no difference in GDNF, NGF, or RET mRNAs in FTY720-Mitoxy treated WT mice relative to WT Vehicle Baseline (Fig. 4c). When we evaluated FTY720-Mitoxy treated CNP-aSyn Tg mice relative to WT Vehicle Baseline there also was no change in GDNF, NGF, or RET mRNA (Fig. 4d, left side). In contrast, RET mRNA was significantly increased in the sweat pads of FTY720-Mitoxy treated CNP-aSyn Tg mice compared to Tg Vehicle Baseline (Fig. 4d, right side, $p = .0008$), suggesting that MSA-like autonomic sweating dysfunction was significantly improved by FTY720-Mitoxy.

3.5. FTY720-Mitoxy modulates GDNF and GDNF-associated miRNA in CNP-aSyn Tg brain

As mentioned above, we and others find that FTY720 reduces neurodegeneration by increasing BDNF *in vitro* and *in vivo* (Deogracias et al., 2012; Di Pardo et al., 2014; Doi et al., 2013; Efstathopoulos et al., 2015; Fukumoto et al., 2014; Hait et al., 2014; Heinen et al., 2015; Miguez et al., 2015; Noda et al., 2013; Potenza et al., 2016; Ren et al., 2017; Schuhmann et al., 2016; Segura-Ulate et al., 2017b; Vargas-Medrano et al., 2014; Vidal-Martinez et al., 2016). Similarly, FTY720 increases GDNF expression in glial cells (Janssen et al., 2015; Noda et al., 2013). Moreover, BDNF and GDNF loss occurs in parallel with

motor dysfunction in MBP-aSyn Tg brains (Ubhi et al., 2012; Ubhi et al., 2010), and altered BDNF and GDNF expression also occurs in PLP-aSyn Tg brain (Refolo et al., 2018). Regarding FTY720-Mitoxy, it can increase BDNF in MN9D neuronal and in OLN-93 oligodendrocyte cell lines (Vargas-Medrano et al., 2014; Vargas-Medrano et al., 2019), but *in vivo* studies had not been performed.

We measured brain BDNF and GDNF from dissected frontal cortex with underlying corpus callosum, which is enriched in oligodendrocytes in representative WT (N = 12) and CN-PaSyn Tg mice (N = 12) treated with Vehicle or FTY720-Mitoxy. No difference was seen for BDNF (Supplemental Fig. S1). In contrast, GDNF protein increased in FTY720-Mitoxy treated Tg mice above levels seen for Vehicle or FTY720-Mitoxy treated WT mice or Vehicle treated Tg littermates (Fig. 5b, One way ANOVA, p = .027). Similarly, GDNF mRNA was significantly increased in Tg frontal cortex after FTY720-Mitoxy compared to Vehicle treated WT mice (Fig. 5c, left whisker box, p = .0007) or Vehicle treated Tg mice (Fig. 5c, right whisker box, p = .0004). As GDNF is downregulated in human MSA, MBP-aSyn Tg mice, and PLP-aSyn Tg mice (Kawamoto et al., 2000; Ubhi et al., 2012; Ubhi et al., 2010) we were surprised to see that this did not occur in our Vehicle treated CNP-aSyn Tg mice (Fig. 5b).

The opposite has been shown for miR-96–5p, which is upregulated in human MSA and MBP-aSyn Tg brain (Ubhi et al., 2014), an upregulation that would decrease GDNF expression. Remarkably, no evaluation of miR-96–5p or GDNF has been directly studied in the context of MSA, despite evidence that miR-96–5p regulates GDNF mRNA through octamer (8-mer) sequences with perfect complementarity in miR-96–5p and the G NF 3’-untranslated region 3’UTR) (Kumar et al., 2015) (Fig. 5e). We thus measured miR-96–5p in frontal cortex of Vehicle treated WT and Tg mice, and noted that baselines did not differ (Fig. 5d), suggesting CNP-aSyn Tg mice do not suffer miR-96–5p dysregulation, consistent with their normal GDNF protein levels (Fig. 5b). Nonetheless, in FTY720-Mitoxy treated Tg mice there was a significant decrease in miR-96–5p compared to WT baseline (Fig. 5d, left whisker box, p = .03) and to Tg baseline (Fig. 5d, right whisker box, p = .02). These findings appear to be meaningful and suggest that FTY720-Mitoxy may directly decrease miR-96–5p to increase GDNF mRNA and protein, which could be beneficial for MSA patients.

3.6. FTY720-Mitoxy reduces insoluble aSyn accumulation in CNP-aSyn Tg mice

As CNP-aSyn Tg mice express human WT aSyn only in myelinating cells (Yazawa et al., 2005), we were not surprised to find similar total aSyn protein levels when we evaluated representative WT (N = 3) and Tg (N = 6) lumbar spinal cords by immunoblot (Fig. 6a, 6b, One way ANOVA, p = .232, ns). Similar findings in these mice have previously been reported (Yazawa et al., 2005). To assess pathological aSyn in lumbar spinal cord we sequentially extracted proteins (as detailed in Materials and methods) to isolate soluble aSyn in the first three buffers (HS, HST, and RIPA) and insoluble aSyn in the final buffer (SDS/Urea) of Vehicle and FTY720-Mitoxy treated mice using established methods (Lou et al., 2010; Vidal-Martinez et al., 2016; Wu et al., 2012). Like Yazawa et al. (2005), we also found insoluble monomeric aSyn in SDS-Urea extracts of lumbar spinal cord in WT and Tg mice

(Fig. 6c, white boxed areas). As expected, insoluble aSyn levels were low in WT mice (Fig. 6c, WT Vehicle, 14.9 au) but we also found little insoluble aSyn in FTY720-Mitoxy treated Tg mice (Fig. 6c, Tg FTY720-Mitoxy, 12.8 au). In contrast, Vehicle treated Tg mice had 5 × more insoluble aSyn in lumbar spinal cord (Fig. 6c, Tg Vehicle, 66.2 au) than Tg littermates treated with FTY720-Mitoxy, revealing meaningful differences between conditions. As an independent measure, we also calculated the ratios of insoluble (SDS/Urea) to soluble (HS, HST, RIPA) aSyn from Vehicle treated WT mice (0.33), Vehicle treated Tg mice (0.90), and FTY720-Mitoxy treated Tg mice (0.35), which revealed ~3 × more insoluble aSyn in MSA-like Vehicle treated Tg mice. By inference these data reveal that the bulk of aSyn present in lumbar spinal cord of FTY720-Mitoxy treated Tg mice was soluble, suggesting that FTY720-Mitoxy has the capacity to reverse aSyn aggregation. We performed linear regression to compare aSyn pathology and sweat behavior in 11.5 mo mice and found that when aSyn aggregation increased in lumbar spinal cord, hind paw sweat function became more impaired revealing a significant negative correlation (Fig. 6d).

3.7. Microglial activation in CNP-aSyn Tg cerebellum is reduced by FTY720-Mitoxy

In MSA, inflammation is associated with microglial activation as measured by the microglial marker Iba1 (Kiely et al., 2018; Raj et al., 2017; Waller et al., 2019; Xie et al., 2013). As cerebellar pathology is also common in MSA (Ishizawa et al., 2004), we assessed microglial activation in cerebellar white matter. On dot blots prepared from cerebellar white matter (Fig. 7a) we saw that WT Vehicle treated mice ($\overline{X} \pm SD = 1.0 \pm .12$), WT FTY720-Mitoxy mice ($\overline{X} \pm SD = .98 \pm .24$) and FT 20-Mitoxy treated Tg mice ($\overline{X} \pm SD = 1.06 \pm .20$) had significantly less Iba1 signal than CNP-aSyn Tg mice treated with Vehicle ($\overline{X} \pm SD = 1.73 \pm .19$) (one way ANOVA, p = .0038). Similarly using Iba1 immunohistochemistry, we saw ramified processes on activated microglia in Vehicle treated Tg cerebellar white matter (Fig. 7, bottom left) which was not seen in WT Vehicle (Fig. 7, top left), WT FTY720-Mitoxy (Fig. 7, top right), and FTY720-Mitoxy treated Tg littermates (Fig. 7, bottom right). These findings show that FTY720-Mitoxy has potent anti-inflammatory effects *in vivo*, similar to our prior *in vitro* data with neuronal and oligodendroglial cell lines (Vargas-Medrano et al., 2014; Vargas-Medrano et al., 2019).

3.8. FTY720-Mitoxy protects movement and mitochondria in the 3NP MSA mouse model

Cerebellum contributes to balance and coordination, which is often tested by rotarod. We pre-trained 8 mo old mice WT (N = 8) and Tg CNP-aSyn mice (N = 16) on rotarod, then treated at 8.5 mo with Vehicle alone, 3NP alone, double treatment with FTY720-Mitoxy + 3NP, or FTY720-Mitoxy alone (as detailed in Materials and methods). As baselines were very different, we independently assessed the movement of WT separately from CNP-aSyn Tg mice. In WT mice, we saw meaningful differences between treatments (Fig. 8a, left graph, One way ANOVA, p = .00009). Tukey multiple comparisons revealed that WT Vehicle mice ($\overline{X} \pm SD = 118.8 \pm 22.18$) did ~14 × better than 3NP treated WT mice ($\overline{X} \pm SD = 8.3 \pm 5.6,\ p = .00009$), 3 × better than doubly treated FTY720-Mitoxy + 3NP WT mice ($\overline{X} \pm SD = 36.8 \pm 20.3,\ p = .00008$), and similar to WT FTY720-Mitoxy mice ($\overline{X} \pm SD = 96.17 \pm 27.9,\ p = .14,\ ns$). The CNP-aSyn Tg mice also showed meaningful differences between treatments (Fig. 8a, right graph, One way ANOVA, p = .00008). Tukey

multiple comparisons revealed poor baseline rotarod times in Vehicle treated Tg mice ($\overline{X} \pm SD = 57.9 \pm 31.6$), that were still ~4 × better than 3 NP treated Tg mice ($\overline{X} \pm SD = 15.83 \pm 5.2$, $p = .0003$), very similar to Tg mice doubly treated with FTY720-Mitoxy + 3NP ($\overline{X} \pm SD = 42.6 \pm 29.1$, $p = .37$, ns). Significant improvement was noted in FTY720-Mitoxy treated Tg mice ($\overline{X} \pm SD = 105.3 \pm 17.9$, $p = .00007$). In fact, FTY720-Mitoxy Tg mice moved similarly to WT Vehicle treated mice (FTY720-Mitoxy Tg, 105.3 ± 17.9; WT Vehicle 118.8 ± 22.18, Student's t test, p = .18, ns), confirming that FTY720-Mitoxy reversed the existing motor impairment (Fig. 8a, compare left and right graphs) as seen above in FTY720-Mitoxy treated Tg mice (Fig. 2b).

We also independently assessed SDH (Complex II) activity in mitochondria from WT and CNP-aSyn Tg mice. This was done using purified cerebellar mitochondria from representative WT (N = 3) and Tg mice (N = 3) to measure SDH activity in mitochondria from mice treated with Vehicle alone, 3NP alone, FTY720-Mitoxy + 3NP, or FTY720-Mitoxy alone. SDH activity differences were seen for WT mice (Fig. 8b, left graph, One way ANOVA, p = .046). Tukey multiple comparisons confirmed that WT Vehicle SDH baseline ($\overline{X} \pm SD = .27 \pm .004$) was 3 × more active than 3NP alone WT mice ($\overline{X} \pm SD = .008 \pm .003$, $p = .002$), similar in FTY720-Mitoxy + 3NP doubly treated WT mice ($\overline{X} \pm SD = .031 \pm .003$, $p = .77$, ns) and also similar to FTY720-Mitoxy alone treated WT mice ($\overline{X} \pm SD = .031 \pm .006$, $p = .72$, ns). Meaningful differences in mitochondrial SDH activity were also noted for CNP-aSyn Tg mice (Fig. 8b, right graph, One way ANOVA, p = .019). Vehicle treated Tg mice had mitochondrial SDH activity ($\overline{X} \pm SD = .043 \pm .011$) that was 3 × more active than 3 NP treated Tg mice ($\overline{X} \pm SD = .014 \pm .007$, $p = .45$), similar to FTY720-Mitoxy + 3NP Tg doubly treated mice ($\overline{X} \pm SD = .029 \pm .009$, $p = .42$, ns) and similar to FTY720-Mitoxy Tg mice ($\overline{X} \pm SD = .058 \pm .016$, $p = .31$, ns). Taken together, the 3NP data suggest that FTY720-Mitoxy was able to protect both movement and mitochondria in WT and CNP-aSyn Tg mice.

Discussion

The Food and Drug Administration (FDA) Orphan Products Grants Program encourages development of drugs to treat orphan disorders such as MSA (Orphanet, ORPHA:102), and treatments that enhance trophic factor expression are considered to be broadly protective (Cai et al., 2014). To this end, we created FTY720-Mitoxy and assessed its therapeutic potential using behavioral tests and evaluation of a variety of tissues from WT and CNP-aSyn Tg MSA mice. FTY720-Mitoxy proved to be beneficial at counteracting several MSA-like impairments. Importantly, WT and Tg mice treated with FTY720-Mitoxy showed no apparent adverse effects at doses comparable to those use with the parent compound FTY720. For further clarity regarding our findings, we also summarize the rationale for using various tissues and behaviors and related results in WT and Tg mice treated with FTY720-Mitoxy (Table 1).

As movement is impaired in humans suffering with MSA and also in MSA mouse models, we assessed WT and CNP-aSyn Tg mice rotarod performance before and after treating mice with Vehicle or FTY720-Mitoxy. We reconfirmed the findings of Yazawa et al. (2005) for 6

mo old WT and CNP-aSyn Tg mice, seeing similar rotarod performance at this stage (not shown). After FTY720-Mitoxy, Tg mice that had been impaired at 8 mo (Fig. 2a) were able to stay on the rotarod ~25% longer than their Vehicle treated Tg littermates by 10 – 11.5 mo of age (Fig. 2b, 2c). As muscle wasting is common in MSA (Rehman, 2001) and as exercise can increase soleus muscle mass (Sakakima et al., 2004), we also compared soleus muscles in WT and Tg mice. FTY720-Mitoxy Tg mouse soleus muscles weighed ~20% more than soleus muscles from Vehicle treated Tg MSA littermates. FTY720-Mitoxy treated Tg mice also performed similarly to WT mice treated with Vehicle or FTY720-Mitoxy (Fig. 3). Because FTY720-Mitoxy stimulates trophic factors expression, as does exercise (Cohen et al., 2003; Cotman and Berchtold, 2002; Smith and Zigmond, 2003), we measured BDNF, GDNF, NGF, and RET (GDNF receptor) mRNAs in brain, in regions studied in MBP-aSyn MSA mice. Although BDNF was unchanged (Supplemental Fig. S1), GDNF protein and mRNA were increased in frontal cortex of FTY720-Mitoxy treated Tg mice (Fig. 5a, 5b, 5c).

We also found that levels of miR-96–5p, a modulator of GDNF, were significantly reduced in FTY720-Mitoxy treated Tg mice (Fig. 5d). As with other complementary mRNA/micro RNA interactions, as levels of miR-96–5p go down, levels of GDNF mRNA go up (Kumar et al., 2015). We paid particular attention to miR-96–5p because its expression down-regulates GDNF (Kumar et al., 2015) and because miR-96–5p is upregulated in both human MSA and MBP-aSyn Tg mouse brains (Ubhi et al., 2014). As miR-96–5p contains a perfect 8-mer complementary sequence to the 3'-UTR of GDNF mRNA (Fig. 5e), it typically induces GDNF mRNA degradation. Thus, reducing miR-96–5p likely explains our observed differences in GDNF mRNA and protein in CNP-aSyn Tg mice treated with FTY720-Mitoxy (Fig. 5a, b, c, d). The data suggest that FTY720-Mitoxy contributes to the decrease in miR-96–5p in Tg frontal cortex, which then led to an increase in GDNF expression. This may have occurred by FTY720-Mitoxy directly stimulating a mechanism called "target RNA-directed microRNA degradation" (TDMD) (Fuchs Wightman et al., 2018), although confirmation awaits further study. Nonetheless, if individuals with MSA use a protective drug that can improve movement, muscle mass, and trophic factor expression it should be highly therapeutic.

Autonomic function is dysregulated in MSA, often leading to impaired sweat production and thermoregulation in MSA patients (Coon et al., 2017; Verstappen and Bloem, 2007). As sweating has never been assessed in any MSA models in response to a potential therapeutic, we measured sweating in WT and CNP-aSyn Tg littermates treated with Vehicle or FTY720-Mitoxy. We saw that sweating was similar for Vehicle and FTY720-Mitoxy treated WT mice (Fig. 4b), but significantly impaired in Vehicle treated Tg MSA mice, and significantly improved in Tg littermates treated with FTY720-Mitoxy (Fig. 4a, 4b). During development GDNF, NGF and acetylcholine contribute to normal sweat pad innervation (Grant et al., 1995) and GDNF and the RET receptor are normally present in sweat gland (Yoshida, 2004), thus we measured GDNF, NGF, and the RET receptor expression in sweat pads on the hind paw. There was no change in GDNF or NGF in WT or Tg mice, however, RET receptor mRNA was significantly increased in Tg mice after FTY720-Mitoxy (Fig. 4d), which may have improved sweat gland GDNF signaling to improve sweating, although this also awaits confirmation. Yet, WT mice treated with FTY720-Mitoxy did not have increased

sweating. Thus, a drug that normalizes sweat and thermoregulation for MSA patients should dramatically improve their quality of life.

Both motor and autonomic inputs to the hind limb pass through lumbar spinal cord. Synucleinopathy has already been confirmed in the spinal cord of aging CNP-aSyn Tg mice (Yazawa et al., 2005), thus, we measured pathological insoluble aSyn in Tg mice treated with Vehicle or FTY720-Mitoxy. We found that the MSA-like Tg mice treated with Vehicle had 3 × more insoluble aSyn in lumbar spinal cord than their Tg littermates treated with FTY720-Mitoxy (Fig. 6c). This suggests that FTY720-Mitoxy was able to reverse synucleinopathy, similar to our findings using the parent compound FTY720 in parkinsonian A53T Tg mice (Vidal-Martinez et al., 2016). Because human aSyn expression in CNP-aSyn Tg mice is limited to myelinating oligodendrocytes primarily in the white matter, it was not surprising that aSyn protein levels were similar in frontal cortex of WT and CNP-aSyn Tg mice (Fig. 6a, b) which contains abundant gray matter with endogenous mouse aSyn. However, when we isolated soluble and insoluble aSyn from spinal cord by sequential extraction, insoluble aSyn in SDS/Urea samples of CNP-aSyn Tg mice were highest for Vehicle treated Tg mice (Fig. 6c, middle group), findings that reiterate prior data in this model (Yazawa et al., 2005). Additionally, insoluble aSyn levels were low in FTY720-Mitoxy treated CNP-aSyn Tg mice, similar to their age matched WT littermates (Fig. 6c, compare white boxed regions on aSyn blot). Based on these findings, we conclude that FTY720-Mitoxy reversed or prevented the progressive synucleinopathy in Tg Vehicle lumbar spinal cord from 8.5 – 11. 5 mo. Identifying a therapeutic for MSA that will normalize aSyn solubility could be particularly protective.

We also showed *in vivo* that neuroinflammation in cerebellar white matter was reduced in Tg mice by FTY720-Mitoxy (Fig. 7) by measuring microglial activation associated with Iba1. Thus, although we know that FTY720-Mitoxy is not immunosuppressive in the same manner at FTY720 (Segura-Ulate et al., 2017a), FTY720-Mitoxy did reduce microglia activation raising the possibility that FTY720-Mitoxy may positively regulate microglia-associated immune effects (Graeber and Streit, 2010; Schetters et al., 2018). As microglial activation is very common in MSA, a drug that counteracts this type of neuroinflammation should be protective.

FTY720-Mitoxy was present in the mitochondrial sample as might be expected for a compound with a TPP modification (Fig. 1b, bottom chromatogram) (Zielonka et al., 2017), though TPP compounds can also be found in cytosol (Filipovska et al., 2004), and we have not ruled out if FTY720-Mitoxy may be present in other cellular compartments. To directly test FTY720-Mitoxy effects on mitochondria we evaluated SDH activity in mitochondria obtained from WT and CNP-aSyn Tg cerebellar white matter after treating with the mitochondrial toxin 3NP ± FTY720-Mitoxy. In those studies both WT and CNP-aSyn Tg mice treated with 3NP + FTY720-Mitoxy had preserved SDH activity, demonstrating the drug's ability to protect mitochondria (Fig. 8b). As mitochondria are impaired in MSA, a drug that will protect these organelles should improve oxidative metabolism throughout the body to improve both CNS and PNS function.

Overall, FTY720-Mitoxy emerges as a potential MSA therapeutic that may improve motor function while decreasing synucleinopathy, increasing muscle mass and improving thermoregulation and sweat function. These beneficial effects were associated with reduced miR-96–5p expression and a corresponding increase in the potent neurotrophic molecule, GDNF. Unlike FTY720, which causes overt immunosuppression by reducing circulating T lymphocytes in the blood (Brinkmann, 2009), FTY720-Mitoxy does not affect T cells (Segura-Ulate et al., 2017a), thus making it a potentially safer option for aging disorders like MSA.

Supplementary Material

Refer to Web version on PubMed Central for supplementary material.

Acknowledgments:

We dedicate this work in memory of the victims of the August 3, 2019 shooting in El Paso, and S. M. Hoy, J. Cordy and L. “Rusty” Lanelli. We thank the following for financial support: Fogarty International Center - U.S./Costa Rica Neuropsychiatric Genetics Research Training Program (NCOD-5D43TW008333), Texas Tech University Health Sciences Center El Paso Graduate School of Biomedical Sciences (ISU/RGP), Multiple System Atrophy Coalition (GVM/RGP), Lizanell and Colbert Coldwell Foundation, El Paso Community Foundation, Paso Del Norte Health Foundation, Hoy Family Research, Perez Family Research, and Anna Mae Doyle gift funds (RGP). We also thank our Texas Tech University Health Sciences Center El Paso colleagues in the Center of Emphasis in Neurosciences (COEN), especially Director Dr. Michael Escamilla and Dr. Olof Sundin for their critical reading of the manuscript.

References cited

Ahmed Z, Asi YT, Lees AJ, Revesz T, Holton JL, 2013. Identification and quantification of oligodendrocyte precursor cells in multiple system atrophy, progressive supranuclear palsy and Parkinson’s disease. Brain Pathol 23, 263–273. [PubMed: 22994884]

Alberico SL, Cassell MD, Narayanan NS, 2015. The Vulnerable Ventral Tegmental Area in Parkinson’s isease. Basal ganglia 5, 51–55. [PubMed: 26251824]

Alsemari A, Al-Hindi HN, 2015. Large-scale mitochondrial DNA deletion underlying familial multiple system atrophy of the cerebellar subtype. Clinical case reports 4, 111–117. [PubMed: 26862402]

Aranda PS, LaJoie DM, Jorcyk CL, 2012. Bleach gel: A simple agarose gel for analyzing RNA quality. Electrophoresis 33, 366–369. [PubMed: 22222980]

Ayzenberg I, Hoepner R, Kleiter I, 2016. Fingolimod for multiple sclerosis and emerging indications: appropriate patient selection, safety precautions, and special considerations. Ther Clin Risk Manag 12, 261–272. [PubMed: 26929636]

Blin, Desnuelle C, Rascol, Borg M, Peyro Saint Paul H, Azulay JP, Bille F, Figarella D, Coulom F, Pellissier JF, Montrastruc JL, Chatel M, Serratrice G, 1994. Mitochondria respiratory failure in skeletal muscle from patients with Parkinson’s disease and multiple system atrophy. J Neurolog Sci 125, 95–101.

Brinkmann V, 2009. FTY720 (fingolimod) in Multiple Sclerosis: therapeutic effects in the immune and the central nervous system. British journal of pharmacology 158, 1173–1182. [PubMed: 19814729]

Cai J, Hua F, Yuan L, Tang W, Lu J, Yu S, Wang X, Hu Y, 2014. Potential therapeutic effects of neurotrophins for acute and chronic neurological diseases. BioMed research international 2014, 601084–601084. [PubMed: 24818146]

Chiba K, Yanagawa Y, Masubuchi Y, Kataoka H, Kawaguchi T, Ohtsuki M, Hoshino Y, 1998. FTY720, a novel immunosuppressant, induces sequestration of circulating mature lymphocytes by acceleration of lymphocyte homing in rats. I. FTY720 selectively decreases the number of circulating mature lymphocytes by acceleration of lymphocyte homing. J Immunol 160, 5037–5044. [PubMed: 9590253]

Chinnasamy R, Nayak TK, Burai R, Dennis MK, Hathaway HJ, Sklar LA, Prossnitz ER, Arterburn JB, 2010. Synthesis and Characterization of Iodinated Tetrahydroquinolines Targeting the G Protein-Coupled Estrogen Receptor GPR30. Journal of medicinal chemistry 53, 1004–1014. [PubMed: 20041667]

Christianson JA, Riekhof JT, Wright DE, 2003. Restorative effects of neurotrophin treatment on diabetes-induced cutaneous axon loss in mice. Experimental neurology 179, 188–199. [PubMed: 12618126]

Cohen AD, Tillerson JL, Smith AD, Schallert T, Zigmond MJ, 2003. Neuroprotective effects of prior limb use in 6-hydroxydopamine-treated rats: possible role of GDNF. J Neurochem 85, 299–305. [PubMed: 12675906]

Coon EA, Fealey RD, Sletten DM, Mandrekar JN, Benarroch EE, Sandroni P, Low PA, Singer W, 2017. Anhidrosis in Multiple System Atrophy Involves Pre- and Postganglionic Sudomotor Dysfunction. Movement disorders : official journal of the Movement Disorder Society 32, 397–404. [PubMed: 27859565]

Cotman CW, Berchtold NC, 2002. Exercise: a behavioral intervention to enhance brain health and plasticity. Trends in neurosciences 25, 295–301. [PubMed: 12086747]

Crupi AN, Nunnelee JS, Taylor DJ, Thomas A, Vit J-P, Riera CE, Gottlieb RA, Goodridge HS, 2018. Oxidative muscles have better mitochondrial homeostasis than glycolytic muscles throughout life and maintain mitochondrial function during aging. Aging 10, 3327–3352. [PubMed: 30449736]

Deogracias R, Yazdani M, Dekkers MP, Guy J, Ionescu MC, Vogt KE, Barde YA, 2012. Fingolimod, a sphingosine-1 phosphate receptor modulator, increases BDNF levels and improves symptoms of a mouse model of Rett syndrome. Proc Natl Acad Sci U S A 109, 14230–14235. [PubMed: 22891354]

Di Pardo A, Amico E, Favellato M, Castrataro R, Fucile S, Squitieri F, Maglione V, 2014. FTY720 (fingolimod) is a neuroprotective and disease-modifying agent in cellular and mouse models of Huntington disease. Human molecular genetics 23, 2251–2265. [PubMed: 24301680]

Dickson DW, Lin W, Liu WK, Yen SH, 1999. Multiple system atrophy: a sporadic synucleinopathy. Brain Pathol 9, 721–732. [PubMed: 10517510]

Doi Y, Takeuchi H, Horiuchi H, Hanyu T, Kawanokuchi J, Jin S, Parajuli B, Sonobe Y, Mizuno T, Suzumura A, 2013. Fingolimod phosphate attenuates oligomeric amyloid beta-induced neurotoxicity via increased brain-derived neurotrophic factor expression in neurons. PLoS One 8, e61988. [PubMed: 23593505]

Efstathopoulos P, Kourgiantaki A, Karali K, Sidiropoulou K, Margioris AN, Gravanis A, Charalampopoulos I, 2015. Fingolimod induces neurogenesis in adult mouse hippocampus and improves contextual fear memory. Translational psychiatry 5, e685. [PubMed: 26795749]

Enoru JO, Yang B, Krishnamachari S, Villanueva E, DeMaio W, Watanyar A, Chinnasamy R, Arterburn JB, Perez RG, 2016. Preclinical Metabolism, Pharmacokinetics and In Vivo Analysis of New Blood-Brain-Barrier Penetrant Fingolimod Analogues: FTY720-C2 and FTY720-Mitoxy. PLoS One 11, e0162162. [PubMed: 27611691]

Fanciulli A, Wenning GK, 2015. Multiple-system atrophy. The New England journal of medicine 372, 249–263. [PubMed: 25587949]

Filipovska A, Eccles MR, Smith RAJ, Murphy MP, 2004. Delivery of antisense peptide nucleic acids (PNAs) to the cytosol by disulphide conjugation to a lipophilic cation. FEBS letters 556, 180–186. [PubMed: 14706847]

Fuchs Wightman F, Giono LE, Fededa JP, de la Mata M, 2018. Target RNAs Strike Back on MicroRNAs. Frontiers in genetics 9.

Fukumoto K, Mizoguchi H, Takeuchi H, Horiuchi H, Kawanokuchi J, Jin S, Mizuno T, Suzumura A, 2014. Fingolimod increases brain-derived neurotrophic factor levels and ameliorates amyloid beta-induced memory impairment. Behavioural brain research 268, 88–93. [PubMed: 24713151]

Giasson BI, Duda JE, Quinn SM, Zhang B, Trojanowski JQ, Lee VM, 2002. Neuronal alpha-synucleinopathy with severe movement disorder in mice expressing A53T human alpha-synuclein. Neuron 34, 521–533. [PubMed: 12062037]

Giasson BI, Forman MS, Higuchi M, Golbe LI, Graves CL, Kotzbauer PT, Trojanowski JQ, Lee VM, 2003. Initiation and synergistic fibrillization of tau and alpha-synuclein. Science 300, 636–640. [PubMed: 12714745]

Graeber MB, Streit WJ, 2010. Microglia: biology and pathology. Acta neuropathologica 119, 89–105. [PubMed: 20012873]

Graham DR, Sidhu A, 2010. Mice expressing the A53T mutant form of human alpha-synuclein exhibit hyperactivity and reduced anxiety-like behavior. Journal of neuroscience research 88, 1777–1783. [PubMed: 20077428]

Grant MP, Francis NJ, Landis SC, 1995. The role of acetylcholine in regulating secretory responsiveness in rat sweat glands. Molecular and cellular neurosciences 6, 32–42. [PubMed: 7599957]

Hait NC, Wise LE, Allegood JC, O'Brien M, Avni D, Reeves TM, Knapp PE, Lu J, Luo C, Miles MF, Milstien S, Lichtman AH, Spiegel S, 2014. Active, phosphorylated fingolimod inhibits histone deacetylases and facilitates fear extinction memory. Nature neuroscience 17, 971–980. [PubMed: 24859201]

Heinen A, Beyer F, Tzekova N, Hartung HP, Kury P, 2015. Fingolimod induces the transition to a nerve regeneration promoting Schwann cell phenotype. Experimental neurology 271, 25–35. [PubMed: 25957629]

Ishizawa K, Komori T, Sasaki S, Arai N, Mizutani T, Hirose T, 2004. Microglial Activation Parallels System Degeneration in Multiple System Atrophy. Journal of Neuropathology & Experimental Neurology 63, 43–52.

Janssen S, Schlegel C, Gudi V, Prajeeth CK, Skripuletz T, Trebst C, Stangel M, 2015. Effect of FTY720-phosphate on the expression of inflammation-associated molecules in astrocytes in vitro. Mol Med Rep 12, 6171–6177. [PubMed: 26239526]

Jecmenica-Lukic M, Poewe W, Tolosa E, Wenning GK, 2012. Premotor signs and symptoms of multiple system atrophy. Lancet neurology 11, 361–368. [PubMed: 22441197]

Jellinger KA, 2014. Neuropathology of multiple system atrophy: new thoughts about pathogenesis. Movement disorders : official journal of the Movement Disorder Society 29, 1720–1741. [PubMed: 25297524]

Jellinger KA, 2016. Recent advances in multiple system atrophy. Journal of Neurology & Neuromedicine 1, 6–17. [PubMed: 27796011]

Jellinger KA, Seppi K, Wenning GK, 2005. Grading of neuropathology in multiple system atrophy: proposal for a novel scale. Movement disorders : official journal of the Movement Disorder Society 20 Suppl 12, S29–36. [PubMed: 16092088]

Kahle PJ, Neumann M, Ozmen L, Muller V, Jacobsen H, Spooren W, Fuss B, Mallon B, Macklin WB, Fujiwara H, Hasegawa M, Iwatsubo T, Kretzschmar HA, Haass C, 2002. Hyperphosphorylation and insolubility of alpha-synuclein in transgenic mouse oligodendrocytes. EMBO reports 3, 583–588. [PubMed: 12034752]

Kawamoto Y, Nakamura S, Akiguchi I, Kimura J, 1999. Increased brain-derived neurotrophic factor-containing axons in the basal ganglia of patients with multiple system atrophy. Journal of neuropathology and experimental neurology 58, 765–772. [PubMed: 10411346]

Kawamoto Y, Nakamura S, Matsuo A, Akiguchi I, 2000. Glial cell line-derived neurotrophic factor-like immunoreactivity in the cerebella of normal subjects and patients with multiple system atrophy. Acta neuropathologica 100, 131–137. [PubMed: 10963359]

Kiely AP, Murray CE, Foti SC, Benson BC, Courtney R, Strand C, Lashley T, Holton JL, 2018. Immunohistochemical and Molecular Investigations Show Alteration in the Inflammatory Profile of Multiple System Atrophy Brain. Journal of neuropathology and experimental neurology 77, 598–607. [PubMed: 29850876]

Kihara M, Sugenoya J, Takahashi A, 1991. The assessment of sudomotor dysfunction in multiple system atrophy. Clinical autonomic research : official journal of the Clinical Autonomic Research Society 1, 297–302. [PubMed: 1822263]

Kumar A, Kopra J, Varendi K, Porokuokka LL, Panhelainen A, Kuure S, Marshall P, Karalija N, Harma MA, Vilenius C, Lillevali K, Tekko T, Mijatovic J, Pulkkinen N, Jakobson M, Jakobson M, Ola R, Palm E, Lindahl M, Stromberg I, Voikar V, Piepponen TP, Saarma M, Andressoo JO, 2015.

GDNF Overexpression from the Native Locus Reveals its Role in the Nigrostriatal Dopaminergic System Function. PLoS genetics 11, e1005710. [PubMed: 26681446]

Kuzdas-Wood D, Irschick R, Theurl M, Malsch P, Mair N, Mantinger C, Wanschitz J, Klimaschewski L, Poewe W, Stefanova N, Wenning GK, 2015. Involvement of Peripheral Nerves in the Transgenic PLP-alpha-Syn Model of Multiple System Atrophy: Extending the Phenotype. PloS one 10, e0136575. [PubMed: 26496712]

Landis SC, Fredieu JR, Yodlowski M, 1985. Neonatal treatment with nerve growth factor antiserum eliminates cholinergic sympathetic innervation of rat sweat glands. Developmental biology 112, 222–229. [PubMed: 3902536]

Lek S, Vargas-Medrano J, Villanueva E, Marcus B, Godfrey W, Perez RG, 2017. Recombinant alpha-beta- and gamma-Synucleins Stimulate Protein Phosphatase 2A Catalytic Subunit Activity in Cell Free Assays. Journal of visualized experiments : JoVE.

Lipp A, Sandroni P, Ahlskog J, et al., 2009. Prospective differentiation of multiple system atrophy from parkinson disease, with and without autonomic failure. Archives of neurology 66, 742–750. [PubMed: 19506134]

Lou H, Montoya SE, Alerte TN, Wang J, Wu J, Peng X, Hong CS, Friedrich EE, Mader SA, Pedersen CJ, Marcus BS, McCormack AL, Di Monte DA, Daubner SC, Perez RG, 2010. Serine 129 phosphorylation reduces the ability of alpha-synuclein to regulate tyrosine hydroxylase and protein phosphatase 2A in vitro and in vivo. J Biol Chem 285, 17648–17661. [PubMed: 20356833]

May VE, Ettle B, Poehler AM, Nuber S, Ubhi K, Rockenstein E, Winner B, Wegner M, Masliah E, Winkler J, 2014. alpha-Synuclein impairs oligodendrocyte progenitor maturation in multiple system atrophy. Neurobiol Aging 35, 2357–2368. [PubMed: 24698767]

Miguez A, Garcia-Diaz Barriga G, Brito V, Straccia M, Giralt A, Gines S, Canals JM, Alberch J, 2015. Fingolimod (FTY720) enhances hippocampal synaptic plasticity and memory in Huntington's disease by preventing p75NTR up-regulation and astrocyte-mediated inflammation. Human molecular genetics 24, 4958–4970. [PubMed: 26063761]

Miller DW, Cookson MR, Dickson DW, 2004. Glial cell inclusions and the pathogenesis of neurodegenerative diseases. Neuron glia biology 1, 13–21. [PubMed: 16614753]

Minnerop M, Luders E, Specht K, Ruhlmann J, Schimke N, Thompson PM, Chou YY, Toga AW, Abele M, Wullner U, Klockgether T, 2010. Callosal tissue loss in multiple system atrophy--a one-year follow-up study. Movement disorders : official journal of the Movement Disorder Society 25, 2613–2620. [PubMed: 20623690]

Monzio Compagnoni G, Kleiner G, Samarani M, Aureli M, Faustini G, Bellucci A, Ronchi D, Bordoni A, Garbellini M, Salani S, Fortunato F, Frattini E, Abati E, Bergamini C, Fato R, Tabano S, Miozzo M, Serratto G, Passafaro M, Deleidi M, Silipigni R, Nizzardo M, Bresolin N, Comi GP, Corti S, Quinzii CM, Di Fonzo A, 2018. Mitochondrial Dysregulation and Impaired Autophagy in iPSC-Derived Dopaminergic Neurons of Multiple System Atrophy. Stem Cell Reports 11, 1185–1198. [PubMed: 30344007]

Morris MA, Gibb DR, Picard F, Brinkmann V, Straume M, Ley K, 2005. Transient T cell accumulation in lymph nodes and sustained lymphopenia in mice treated with FTY720. European journal of immunology 35, 3570–3580. [PubMed: 16285007]

Nakamura K, Mori F, Kon T, Tanji K, Miki Y, Tomiyama M, Kurotaki H, Toyoshima Y, Kakita A, Takahashi H, Yamada M, Wakabayashi K, 2015. Filamentous aggregations of phosphorylated alpha-synuclein in Schwann cells (Schwann cell cytoplasmic inclusions) in multiple system atrophy. Acta neuropathologica communications 3, 29. [PubMed: 25990096]

Noda H, Takeuchi H, Mizuno T, Suzumura A, 2013. Fingolimod phosphate promotes the neuroprotective effects of microglia. Journal of neuroimmunology 256, 13–18. [PubMed: 23290828]

Overk C, Rockenstein E, Valera E, Stefanova N, Wenning G, Masliah E, 2018. Multiple system atrophy: experimental models and reality. Acta neuropathologica 135, 33–47. [PubMed: 29058121]

Papp MI, Kahn JE, Lantos PL, 1989. Glial cytoplasmic inclusions in the CNS of patients with multiple system atrophy (striatonigral degeneration, olivopontocerebellar atrophy and Shy-Drager syndrome). Journal of the neurological sciences 94, 79–100. [PubMed: 2559165]

Paugh SW, Payne SG, Barbour SE, Milstien S, Spiegel S, 2003. The immunosuppressant FTY720 is phosphorylated by sphingosine kinase type 2. FEBS letters 554, 189–193. [PubMed: 14596938]

Pfaffl MW, Horgan GW, Dempfle L, 2002. Relative expression software tool (REST) for group-wise comparison and statistical analysis of relative expression results in real-time PCR. Nucleic acids research 30, e36. [PubMed: 11972351]

Potenza RL, De Simone R, Armida M, Mazziotti V, Pezzola A, Popoli P, Minghetti L, 2016. Fingolimod: A Disease-Modifier Drug in a Mouse Model of Amyotrophic Lateral Sclerosis. Neurotherapeutics : the journal of the American Society for Experimental NeuroTherapeutics 13, 918–927. [PubMed: 27456702]

Raj D, Yin Z, Breur M, Doorduin J, Holtman IR, Olah M, Mantingh-Otter IJ, Van Dam D, De Deyn PP, den Dunnen W, Eggen BJL, Amor S, Boddeke E, 2017. Increased White Matter Inflammation in Aging- and Alzheimer's Disease Brain. Frontiers in molecular neuroscience 10, 206–206. [PubMed: 28713239]

Refolo V, Bez F, Polissidis A, Kuzdas-Wood D, Sturm E, Kamaratou M, Poewe W, Stefanis L, Angela Cenci M, Romero-Ramos M, Wenning GK, Stefanova N, 2018. Progressive striatonigral degeneration in a transgenic mouse model of multiple system atrophy: translational implications for interventional therapies. Acta neuropathologica communications 6, 2–2. [PubMed: 29298733]

Rehman HU, 2001. Multiple system atrophy. Postgraduate medical journal 77, 379–382. [PubMed: 11375450]

Ren M, Han M, Wei X, Guo Y, Shi H, Zhang X, Perez RG, Lou H, 2017. FTY720 Attenuates 6-OHDA-Associated Dopaminergic Degeneration in Cellular and Mouse Parkinsonian Models. Neurochemical research 42, 686–696. [PubMed: 27943027]

Sakakima H, Yoshida Y, Suzuki S, Morimoto N, 2004. The Effects of Aging and Treadmill Running on Soleus and Gastrocnemius Muscle Morphology in the Senescence-Accelerated Mouse (SAMP1). The Journals of Gerontology: Series A 59, B1015–B1021.

Scallet AC, Nony PL, Rountree RL, Binienda ZK, 2001. Biomarkers of 3-nitropropionic acid (3-NPA)-induced mitochondrial dysfunction as indicators of neuroprotection. Ann N Y Acad Sci 939, 381–392. [PubMed: 11462793]

Schetters STT, Gomez-Nicola D, Garcia-Vallejo JJ, Van Kooyk Y, 2018. Neuroinflammation: Microglia and T Cells Get Ready to Tango. Frontiers in Immunology 8.

Schuhmann MK, Krstic M, Kleinschnitz C, Fluri F, 2016. Fingolimod (FTY720) Reduces Cortical Infarction and Neurological Deficits During Ischemic Stroke Through Potential Maintenance of Microvascular Patency. Curr Neurovasc Res 13, 277–282. [PubMed: 27558201]

Segura-Ulate I, Belcher TK, Vidal-Martinez G, Vargas-Medrano J, Perez RG, 2017a. FTY720-derivatives do not induce FTY720-like lymphopenia. Journal of pharmacological sciences 133, 187–189. [PubMed: 28363412]

Segura-Ulate I, Yang B, Vargas-Medrano J, Perez RG, 2017b. FTY720 (Fingolimod) reverses alpha-synuclein-induced downregulation of brain-derived neurotrophic factor mRNA in OLN-93 oligodendroglial cells. Neuropharmacology 117, 149–157. [PubMed: 28153532]

Shults CW, Rockenstein E, Crews L, Adame A, Mante M, Larrea G, Hashimoto M, Song D, Iwatsubo T, Tsuboi K, Masliah E, 2005. Neurological and neurodegenerative alterations in a transgenic mouse model expressing human alpha-synuclein under oligodendrocyte promoter: implications for multiple system atrophy. The Journal of neuroscience : the official journal of the Society for Neuroscience 25, 10689–10699. [PubMed: 16291942]

Smith AD, Zigmond MJ, 2003. Can the brain be protected through exercise? Lessons from an animal model of parkinsonism☆. Experimental neurology 184, 31–39. [PubMed: 14637076]

Smith PK, Krohn RI, Hermanson GT, Mallia AK, Gartner FH, Provenzano MD, Fujimoto EK, Goeke NM, Olson BJ, Klenk DC, 1985. Measurement of protein using bicinchoninic acid. Analytical biochemistry 150, 76–85. [PubMed: 3843705]

Stefanova N, Puschban Z, Fernagut PO, Brouillet E, Tison F, Reindl M, Jellinger KA, Poewe W, Wenning GK, 2003. Neuropathological and behavioral changes induced by various treatment paradigms with MPTP and 3-nitropropionic acid in mice: towards a model of striatonigral degeneration (multiple system atrophy). Acta neuropathologica 106, 157–166. [PubMed: 12764627]

Stefanova N, Reindl M, Neumann M, Haass C, Poewe W, Kahle PJ, Wenning GK, 2005. Oxidative stress in transgenic mice with oligodendroglial alpha-synuclein overexpression replicates the characteristic neuropathology of multiple system atrophy. The American journal of pathology 166, 869–876. [PubMed: 15743798]

Stefanova N, Reindl M, Neumann M, Kahle P, Poewe W, Wenning G, 2007. Microglial activation mediates neurodegeneration related to oligodendroglial a-synucleinopathy: implications for multiple system atrophy. Movement Disorders 22, 2196–2203. [PubMed: 17853477]

Stefanova N, Wenning GK, 2015. Animal models of multiple system atrophy. Clinical autonomic research : official journal of the Clinical Autonomic Research Society 25, 9–17. [PubMed: 25585910]

Stefanova N, Wenning GK, 2016. Review: Multiple system atrophy: emerging targets for interventional therapies. Neuropathology and applied neurobiology 42, 20–32. [PubMed: 26785838]

Ubhi K, Inglis C, Mante M, Patrick C, Adame A, Spencer B, Rockenstein E, May V, Winkler J, Masliah E, 2012. Fluoxetine ameliorates behavioral and neuropathological deficits in a transgenic model mouse of alpha-synucleinopathy. Experimental neurology 234, 405–416. [PubMed: 22281106]

Ubhi K, Lee PH, Adame A, Inglis C, Mante M, Rockenstein E, Stefanova N, Wenning GK, Masliah E, 2009. Mitochondrial inhibitor 3-nitroproprionic acid enhances oxidative modification of alpha-synuclein in a transgenic mouse model of multiple system atrophy. Journal of neuroscience research 87, 2728–2739. [PubMed: 19405128]

Ubhi K, Low P, Masliah E, 2011. Multiple system atrophy: a clinical and neuropathological perspective. Trends in neurosciences 34, 581–590. [PubMed: 21962754]

Ubhi K, Rockenstein E, Kragh C, Inglis C, Spencer B, Michael S, Mante M, Adame A, Galasko D, Masliah E, 2014. Widespread microRNA dysregulation in multiple system atrophy - disease-related alteration in miR-96. The European journal of neuroscience 39, 1026–1041. [PubMed: 24304186]

Ubhi K, Rockenstein E, Mante M, Inglis C, Adame A, Patrick C, Whitney K, Masliah E, 2010. Neurodegeneration in a transgenic mouse model of multiple system atrophy is associated with altered expression of oligodendroglial-derived neurotrophic factors. The Journal of neuroscience : the official journal of the Society for Neuroscience 30, 6236–6246. [PubMed: 20445049]

Vargas-Medrano J, Krishnamachari S, Villanueva E, Godfrey WH, Lou H, Chinnasamy R, Arterburn JB, Perez RG, 2014. Novel FTY720-based compounds stimulate neurotrophin expression and phosphatase activity in dopaminergic cells. ACS Med Chem Lett 5, 782–786. [PubMed: 25050165]

Vargas-Medrano J, Segura-Ulate I, Yang B, Chinnasamy R, Arterburn JB, Perez RG, 2019. FTY720-mitoxy reduces toxicity associated with alpha-synuclein and oxidative stress by increasing trophic factor expression and myelin protein in OLN-93 oligodendroglia cell cultures. Neuropharmacology 158.

Vargas-Medrano J, Yang B, Garza NT, Segura-Ulate I, Perez RG, 2018. Up-regulation of protective neuronal MicroRNAs by FTY720 and novel FTY720-derivatives. Neuroscience letters 690, 178–180. [PubMed: 30359694]

Verstappen CC, Bloem BR, 2007. Too hot to handle: heat stroke in multiple system atrophy. Journal of neurology 254, 664–665. [PubMed: 17404780]

Vidal-Martinez G, Vargas-Medrano J, Gil-Tommee C, Medina D, Garza NT, Yang B, Segura-Ulate I, Dominguez SJ, Perez RG, 2016. FTY720/Fingolimod reduces synucleinopathy and improves gut motility in A53T Mice: Contributions of pro-brain-derived neurotrophic factor (Pro-BDNF) and mature BDNF. J Biol Chem 291, 20811–20821. [PubMed: 27528608]

Wakabayashi K, Hayashi S, Kakita A, Yamada M, Toyoshima Y, Yoshimoto M, Takahashi H, 1998. Accumulation of alpha-synuclein/NACP is a cytopathological feature common to Lewy body disease and multiple system atrophy. Acta Neuropathol (Berl) 96, 445–452. [PubMed: 9829807]

Waller R, Baxter L, Fillingham DJ, Coelho S, Pozo JM, Mozumder M, Frangi AF, Ince PG, Simpson JE, Highley JR, 2019. Iba-1-/CD68+ microglia are a prominent feature of age-associated deep subcortical white matter lesions. PLOS ONE 14, e0210888. [PubMed: 30682074]

Wasserstein RL, Schirm AL, Lazar NA, 2019. Moving to a World Beyond "p < 0.05". The American Statistician 73, 1–19.

Waxman EA, Giasson BI, 2008. Specificity and regulation of casein kinase-mediated phosphorylation of alpha-synuclein. Journal of neuropathology and experimental neurology 67, 402–416. [PubMed: 18451726]

Wu J, Lou H, Alerte TN, Stachowski EK, Chen J, Singleton AB, Hamilton RL, Perez RG, 2012. Lewy-like aggregation of alpha-synuclein reduces protein phosphatase 2A activity in vitro and in vivo. Neuroscience 207, 288–297. [PubMed: 22326202]

Xie F, Zhang JC, Fu H, Chen J, 2013. Age-related decline of myelin proteins is highly correlated with activation of astrocytes and microglia in the rat CNS. International journal of molecular medicine 32, 1021–1028. [PubMed: 24026164]

Yazawa I, Giasson BI, Sasaki R, Zhang B, Joyce S, Uryu K, Trojanowski JQ, Lee VM, 2005. Mouse model of multiple system atrophy alpha-synuclein expression in oligodendrocytes causes glial and neuronal degeneration. Neuron 45, 847–859. [PubMed: 15797547]

Yoshida T, 2004. Immunohistochemical localization of glial cell line-derived neurotrophic factor and its receptor Ret in the rat sweat gland. The Kurume medical journal 51, 193–202. [PubMed: 15682826]

Yu J, Zhu H, Taheri S, Perry S, Kindy MS, 2018. The Effect of Diet on Improved Endurance in Male C57BL/6 Mice. Nutrients 10, 1101–1111.

Zielonka J, Joseph J, Sikora A, Hardy M, Ouari O, Vasquez-Vivar J, Cheng G, Lopez M, Kalyanaraman B, 2017. Mitochondria-Targeted Triphenylphosphonium-Based Compounds: Syntheses, Mechanisms of Action, and Therapeutic and Diagnostic Applications. Chemical reviews 117, 10043–10120. [PubMed: 28654243]

HIGHLIGHTS

- CNP-aSyn MSA mice develop age-onset motor and sweat dysfunction, synucleinopathy and neuroinflammation
- FTY720-Mitoxy improves movement, muscle mass, and sweat function in MSA mice
- FTY720-Mitoxy reduces MSA mouse synucleinopathy and neuroinflammation
- FTY720-Mitoxy also increases RET and GDNF mRNA while reducing GDNF-modulating miR-96–5p levels

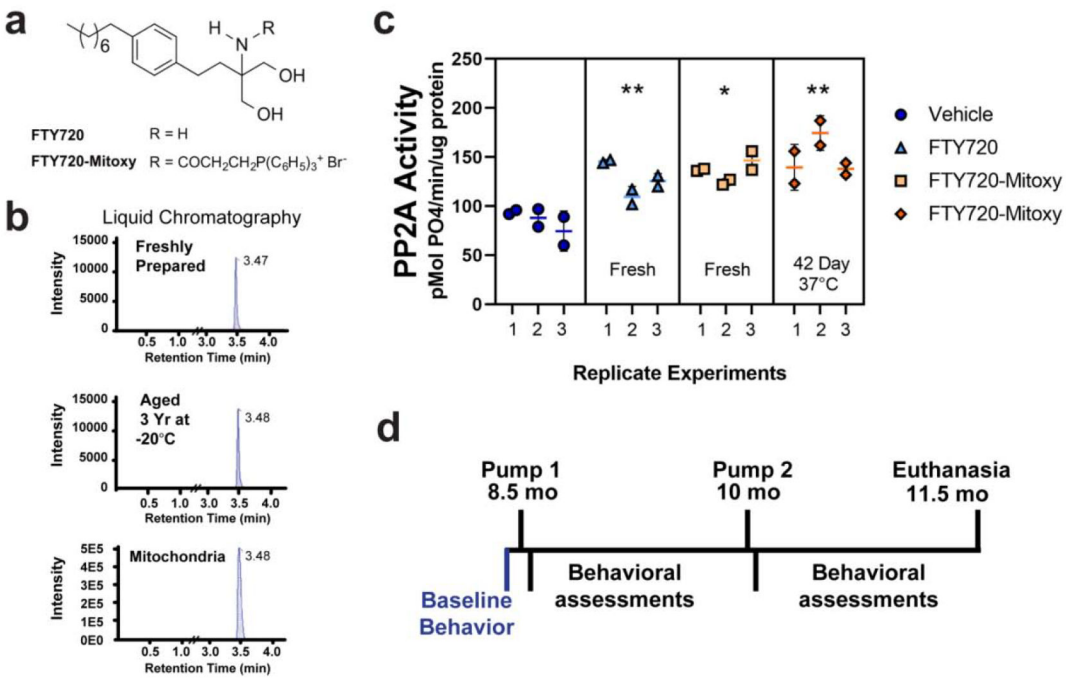

Figure 1. FTY720-Mitoxy is stable in solution, present in mitochondria, and retains activity after long term freezer storage or 42 days at body temperature.

(a) Chemical structures of FTY720 and FTY720-Mitoxy. **(b)** LC-MS/MS shows single peaks, indicating single compounds purified by LC with similar retention times, confirming FTY720-Mitoxy stability when Freshly Prepared, stored 3 years at −20°C, or in mitochondria from FTY720-Mitoxy treated MN9D cells. **(c)** PP2A immunoprecipitated from MN9D cells treated with FTY720 or FTY720-Mitoxy, show similar activation of PP2A in response to fresh FTY720, fresh FTY720-Mitoxy, and FTY720-Mitoxy aged 42 day at 37°C compared to Vehicle. **(d)** Timeline of behavioral assessment and osmotic pump implantation for delivery of Vehicle or FTY720-Mitoxy. Two way repeated measures (RM) ANOVA, * $p < .05$, ** $p < .01$.

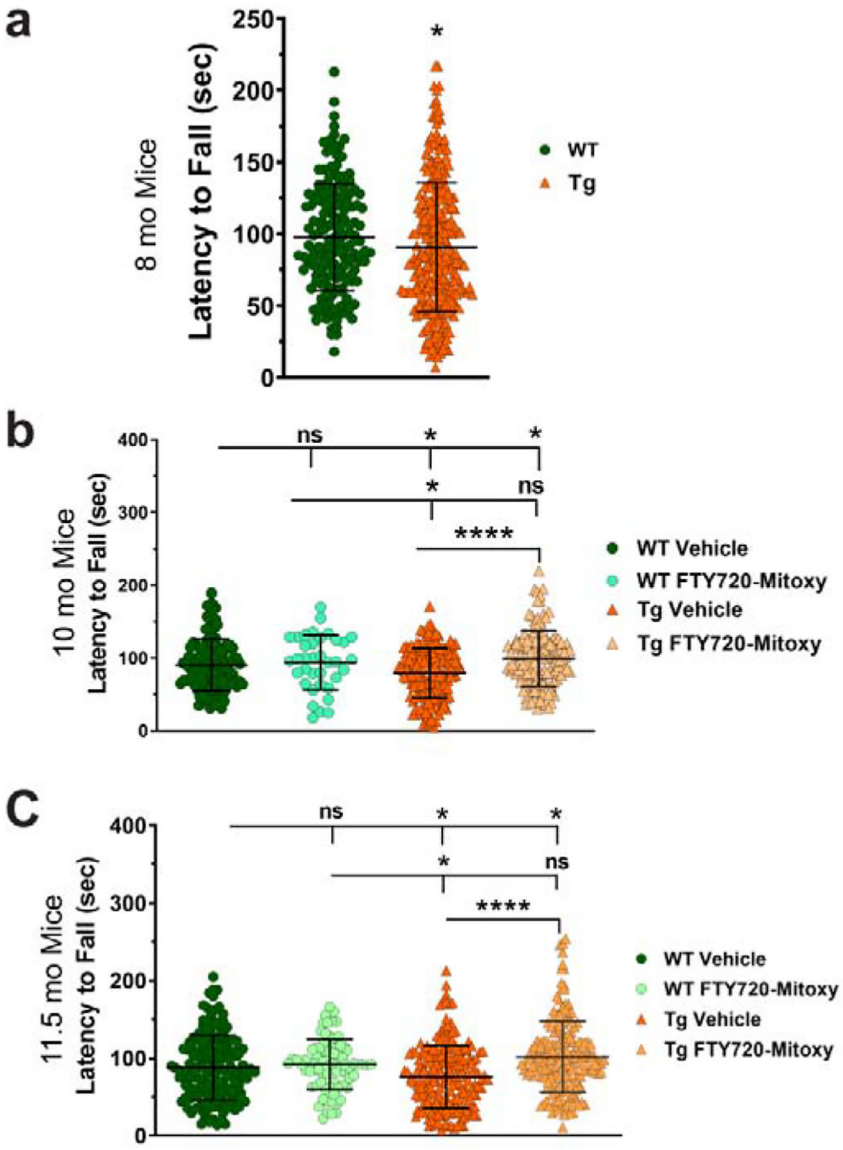

Figure 2. FTY720-Mitoxy reverses motor dysfunction in CNP-aSyn Tg mice.

(a) Baseline rotarod tests prior to pump implantation confirm motor impairment at 8 mo in Tg mice compared to WT littermates. **(b)** At 10 mo, after 42 days of FTY720-Mitoxy or Vehicle, WT mice perform similarly, while Vehicle treated Tg mice were significantly impaired and FTY720-Mitoxy treated Tg mice were significantly improved. **(c)** At 11.5 mo, after 84 days of FTY720-Mitoxy or Vehicle, WT mice show similar performance, while Vehicle treated Tg mice were again impaired and FTY720-Mitoxy treated Tg mice significantly improved. Unpaired t-test and One way ANOVA, * $p < .05$, **** $p < .0001$, ns, not significant.

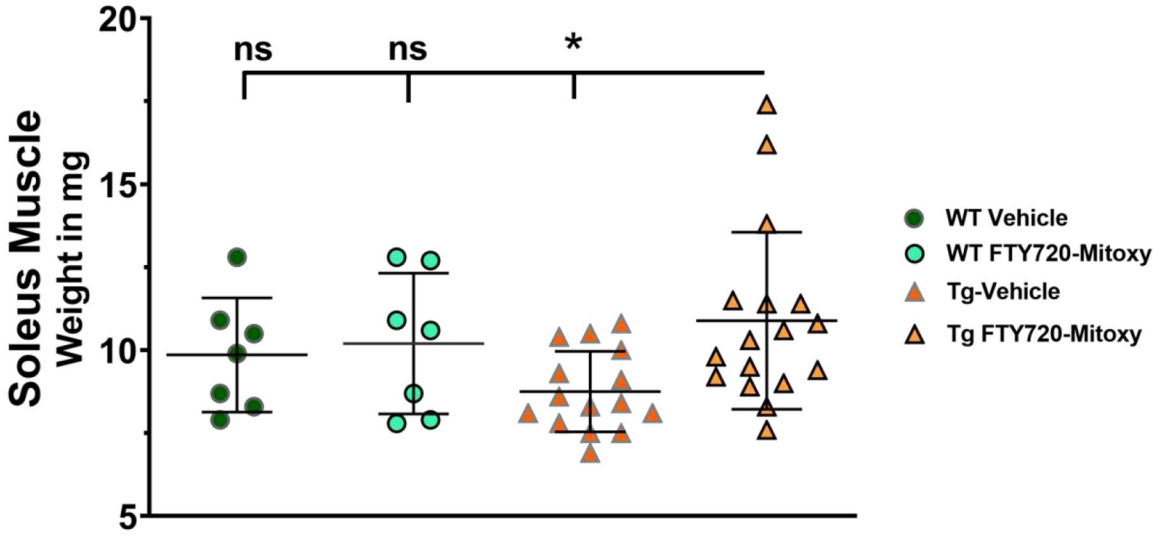

Figure 3. FTY720-Mitoxy increases soleus muscle size in CNP-aSyn Tg mice.

Soleus muscles are larger in FYT720-Mitoxy treated CNP-aSyn Tg mice compared to Vehicle treated Tg littermates, and similar to WT Vehicle or FTY720-Mitoxy treated mice. One way ANOVA, * $p < .05$.

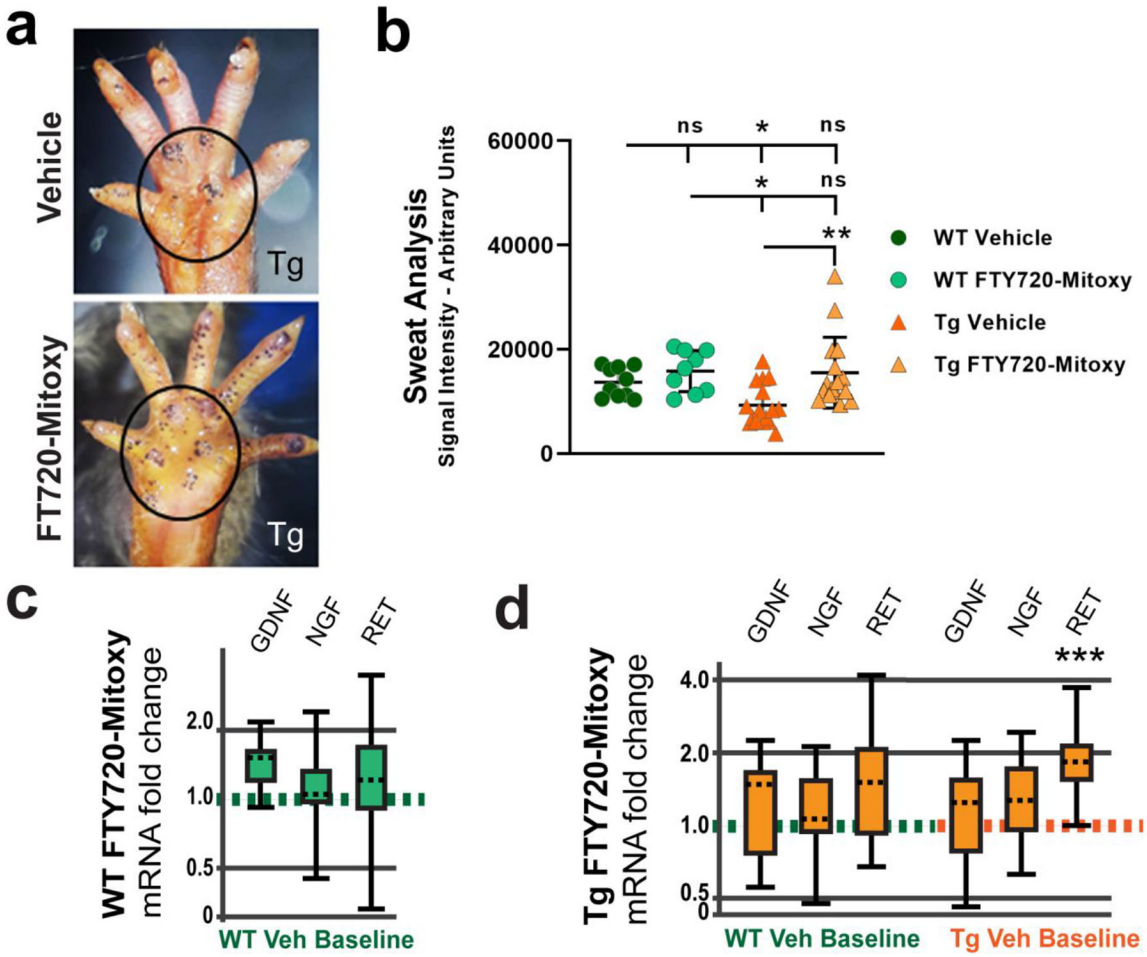

Figure 4. FTY720-Mitoxy improves sweat function in CNP-aSyn Tg MSA mice.

The iodine starch test labels sweat droplets as purple dots on the paw at the 5 min time point. **(a)** Representative images of 11.5 mo old CNP-aSyn Tg mouse treated with Vehicle shows fewer sweat droplets (upper image) than a Tg mouse treated with FTY720-Mitoxy (lower image) with the main paw area outlined. **(b)** Quantification of sweat droplet signal shows more sweat in Tg mice treated with FTY720-Mitoxy as compared to Vehicle treated Tg littermates, and a non-significant trend noted in WT mice treated with FTY720-Mitoxy. One way ANOVA, * $p < .05$. (**c**) Analysis of mRNA by qPCR for WT FTY720-Mitoxy treated mice show no difference in GDNF, NGF, or RET expression relative to WT Vehicle baseline. (**d**) Analysis of mRNA using qPCR shows no difference in GDNF, NGF, or RET mRNA of Tg mice compared to WT Vehicle baseline (left side). In Tg mice compared to Tg Vehicle baseline RET mRNA is significantly increased (right side). The qPCR data were analyzed with REST-2009 suite as detailed in Materials and methods, *** $p < .001$.

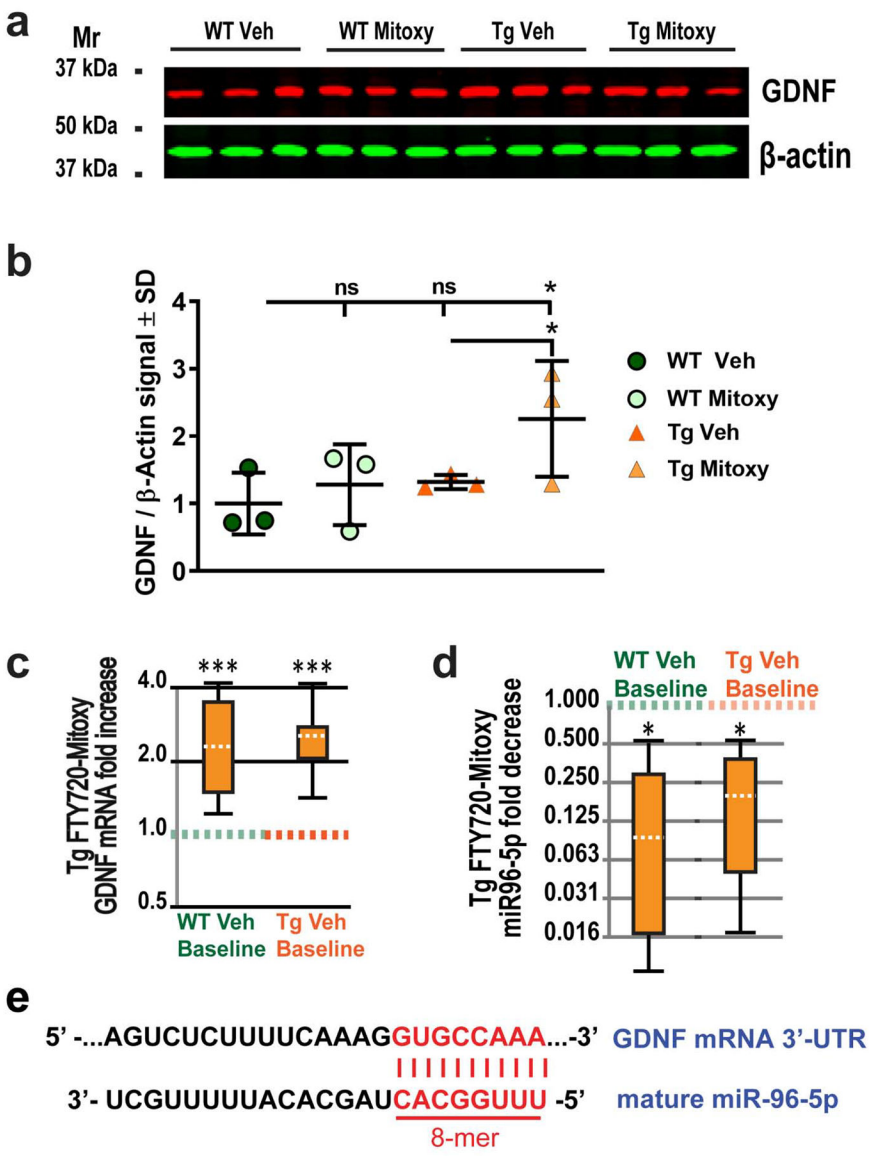

Figure 5. FTY720-Mitoxy increases GDNF protein and mRNA and decreases mature miR-96–5p in CNP-aSyn Tg mice.

(a) GDNF immunoblot of frontal cortex from Vehicle treated WT mice (WT Veh), FTY720-Mitoxy treated WT mice (WT Mitoxy), Vehicle treated CNP-aSyn Tg mice (Tg Veh) or Tg mice treated with FTY720-Mitoxy (Tg Mitoxy). **(b)**. Quantification of G NF/β-actin shows more GDNF protein in Tg FTY720-Mitoxy frontal cortex. One Way ANOVA, * $p < .05$. **(c)**. Analysis of mRNA by qPCR shows more GDNF mRNA in Tg FTY720-Mitoxy treated mice compared to either WT (left whisker box plot) or Tg (right whisker box plot) Vehicle treated mice. **(d)**. Analysis of qPCR shows that FTY720-Mitoxy treated Tg mice also have less miR-96–5p compared to WT (left) or Tg (right) Vehicle treated mice. **(e)**. A perfect 8-mer complementary sequence is shown for mature miR-96–5p and GDNF mRNA 3'-UTR. All qPCR data analyzed using REST-2009 suite, * $p < .05$, *** $p < .001$.

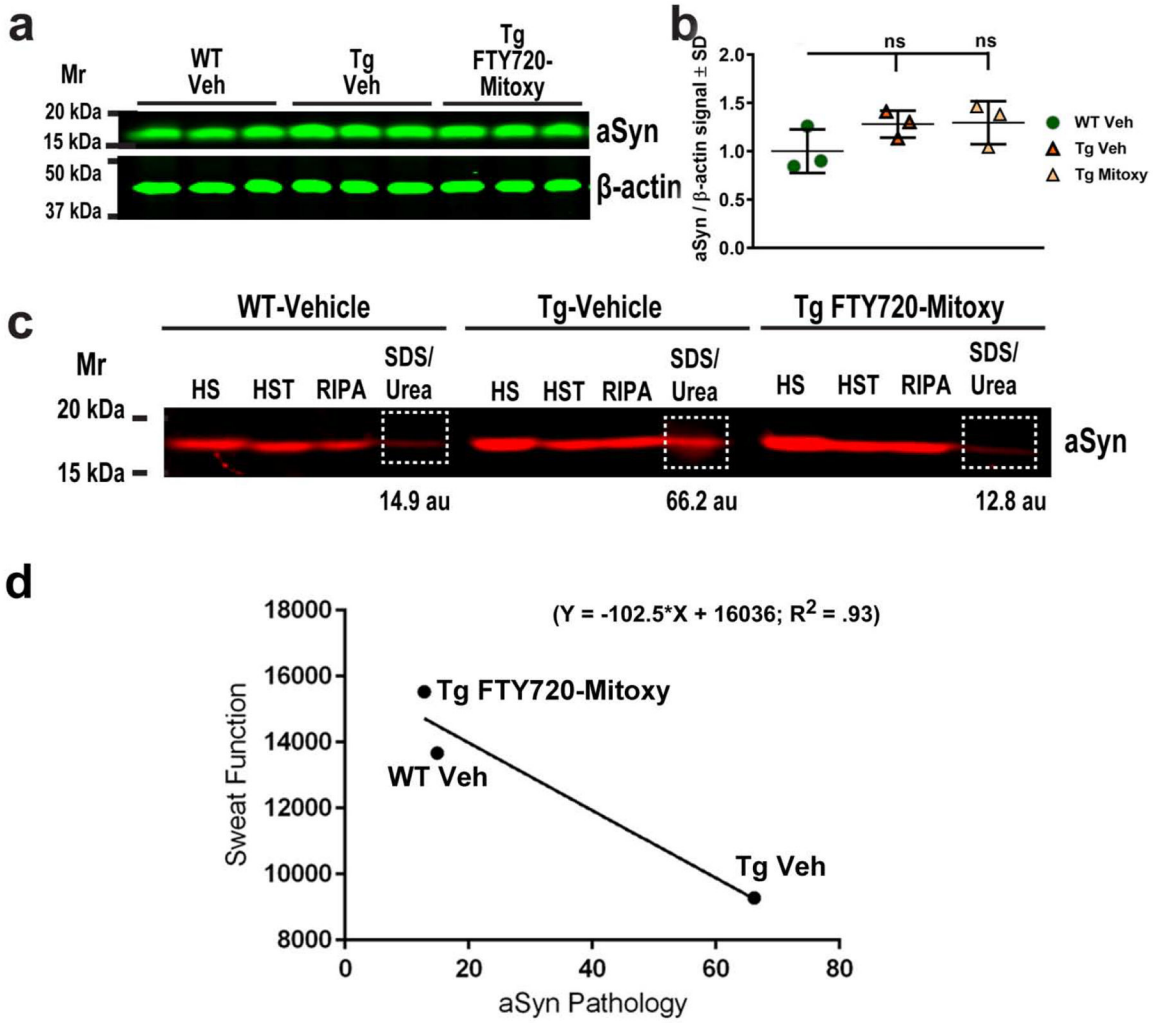

Figure 6. FTY720-Mitoxy reduces insoluble aSyn protein in CNP-aSyn Tg lumbar spinal cord.

(a) Representative aSyn immunoblot of lumbar spinal cord from Vehicle treated WT (WT Veh), Vehicle treated CNP-aSyn Tg (Tg Veh), and FTY720-Mitoxy treated CNP-aSyn Tg mice (Tg FTY720-Mitoxy). (b) aSyn/β-actin quantification confirms similar total aSyn protein levels in all spinal cords. One Way ANOVA, p = .232, ns. (c) Representative immunoblot of soluble and insoluble aSyn from lumbar spinal cord of WT Veh, Tg Veh and FTY720-Mitoxy treated Tg mice. Soluble aSyn is present in High salt (HS), High salt Triton (HST), and RIPA extracts, and insoluble aSyn (outlined in white) is present in SDS/Urea extracts. Levels of Insoluble aSyn are high in Tg Veh and low in WT Veh and Tg FTY720-Mitoxy spinal cords, for signal quantified in arbitrary units (au). (d) Linear regression comparing aSyn pathology and Sweat function reveals a significant negative correlation (R^2 = .93). Tg Veh mice with more aSyn pathology also have more impaired sweat function, while FTY720-Mitoxy Tg mice are comparable to their WT littermates.

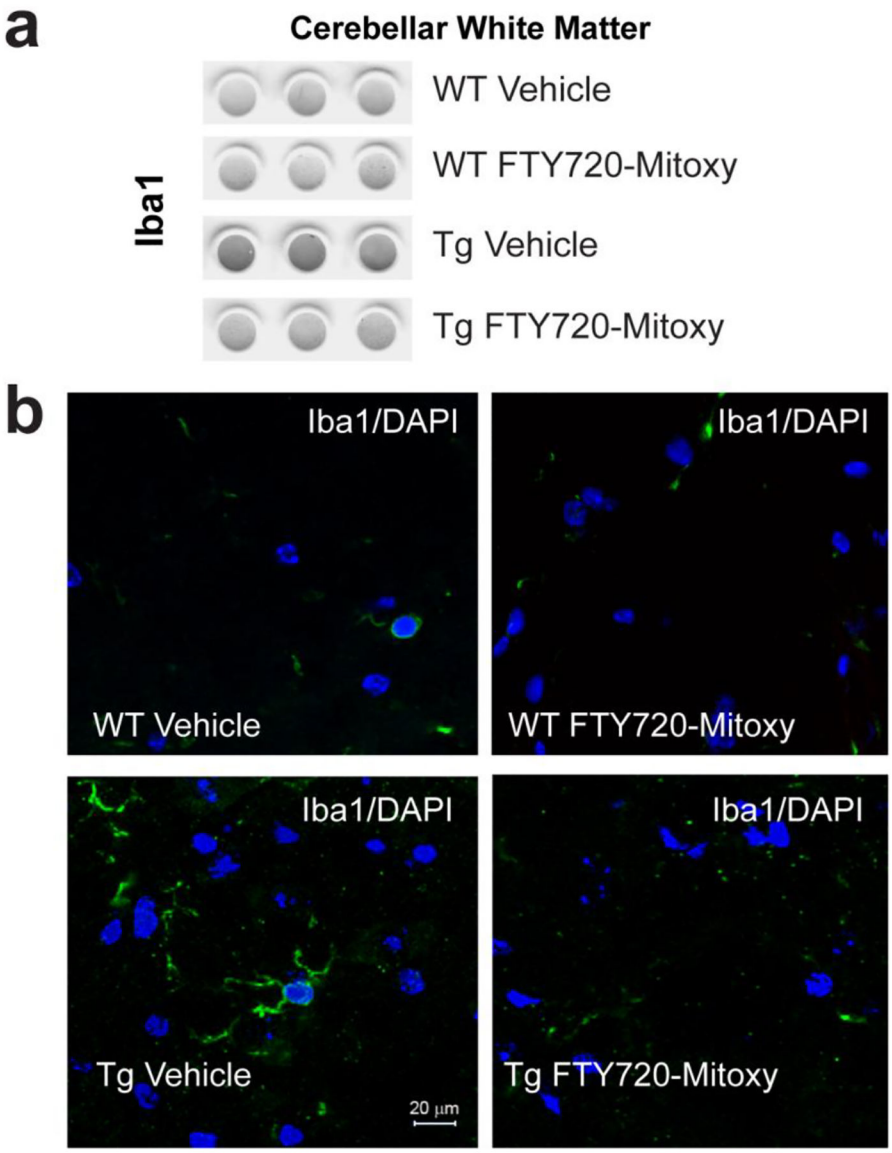

Figure 7. FTY720-Mitoxy decreases microglial activation in cerebellum of CNP-aSyn Tg mice.
(a) Dot blots reacted for Iba1, a microglial marker, show more of this inflammatory marker in cerebellum of Veh Tg mice than in all other conditions. **(b)** Evaluation of cerebellar white matter by immunohistochemistry shows more Iba1 signal (green) present in ramified processes of microglial cells in Veh treated CNP-aSyn MSA mice Tg mice but almost none in WT Vehicle, WT FTY720-Mitoxy, and FTY720-Mitoxy treated Tg MSA mice. DAPI labeled nuclei appear blue in all images. Scale bar = 20 μm

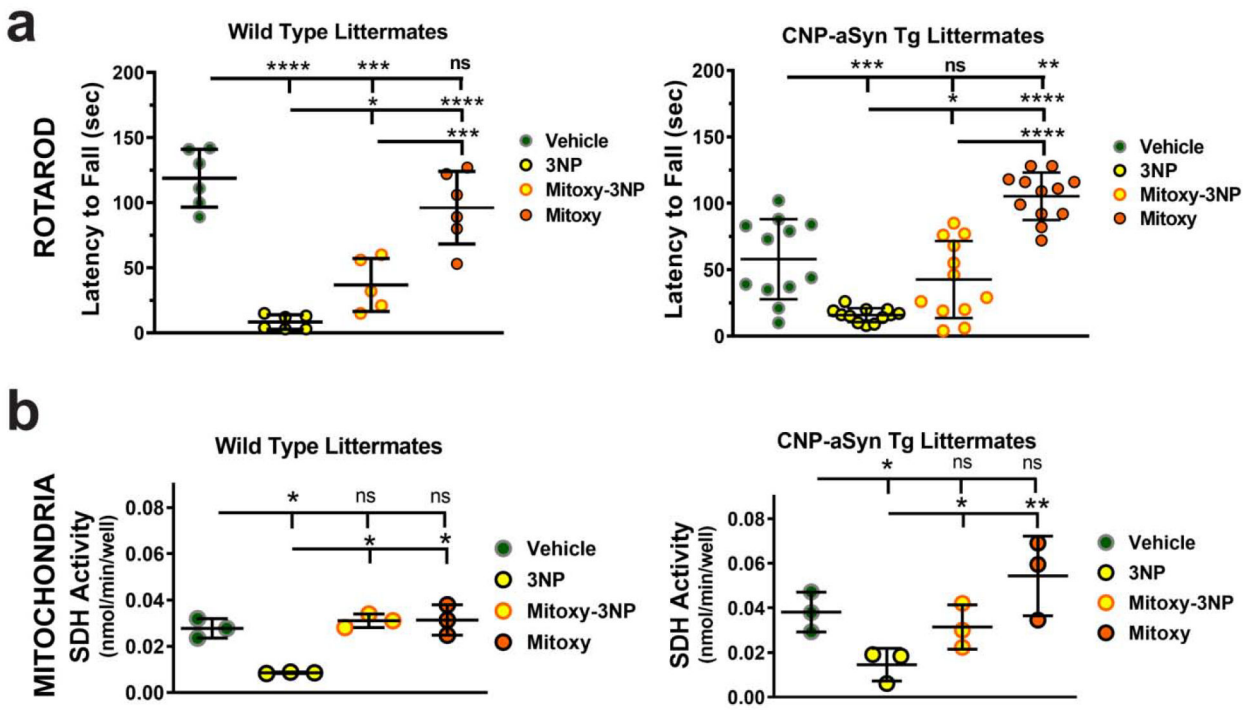

Figure 8. FTY720-Mitoxy inhibits 3NP associated movement and mitochondrial impairment in WT and CNP-aSyn Tg mice.

(a) WT mice (left graph) and CNP-aSyn Tg mice (right graph) rotarod activity in 9 mo mice treated with Vehicle, 3NP alone, FTY720-Mitoxy + 3NP double treatment (Mitoxy-3NP), or FTY720-Mitoxy alone (Mitoxy). Vehicle data show baseline movement. 3NP impaired movement in both WT and CNP-aSyn Tg mice. FTY720-Mitoxy + 3NP double treatment (Mitoxy-3NP) improved above 3NP alone. Treatment with FTY720-Mitoxy restores movement of WT mice and improves movement of CNP-aSyn Tg mice. (b) WT (left graph) and CNP-aSyn Tg (right graph) SDH activity in mitochondria isolated from cerebellum of 9 mo mice treated with Vehicle, 3NP alone, FTY720-Mitoxy + 3NP (Mitoxy-3NP), or FTY720-Mitoxy alone (Mitoxy). Vehicle condition shows baseline SDH activity for WT and CNP-aSyn Tg mitochondria. 3NP reduces SDH activity in WT and CNP-aSyn Tg mitochondria. 3NP + FTY720-Mitoxy double treatment returns SDH activity to baseline values in WT and CNP-aSyn Tg mitochondria as did FTY720-Mitoxy in WT mitochondria, but even more in mitochondria from CNP-aSyn Tg mice. One-way ANOVA, * $p < .05$, ** $p < .01$, *** $p < .001$, **** $p < .0001$, ns, not significant.

Table 1.

Behavior and related effects of FTY720-Mitoxy in aging or 3NP treated WT and CNP-aSyn Tg mice.

Behavior	**Treatment Condition**				**Tissue Tested, Measure Used**	**Rationale**	**Outcome**
Rotarod	**WT Vehicle**	**WT Mitoxy**	**Tg Vehicle**	**Tg Mitoxy**			***Did Mitoxy improve MSA Tg mice?***
Results	Normal **WT** Baseline	Same as **WT** Baseline	Impaired **Tg** Baseline	Improved to **WT** Baseline	Soleus muscle, weight	Bigger muscle better rotarod	**YES**, Tg Mitoxy soleus was bigger
					Frontal Cx, Motor Cx, CC, Trophic factor (TF), miRNA	FTY720-Mitoxy and exercise lead to more TFs	**YES**, Tg Mitoxy more GDNF mRNA, protein, & reduced miR-96–5p
					Cerebellum (Cb), MSA-like inflammation	MSA Cb microglial activation	**YES**, Tg Mitoxy decreased microglia activation
					Lumbar spinal cord, Motor inputs	Tg Spinal cord aSyn pathology	**YES**, Tg Mitoxy reduced Synucleinopathy
Sweat	**WT Vehicle**	**WT Mitoxy**	**Tg Vehicle**	**Tg Mitoxy**			***Did Mitoxy improve MSA Tg mice?***
Results	Normal **WT** Baseline	Same as **WT** Baseline	Impaired **Tg** Baseline	Improved to **WT** Baseline	Sweat pad (hind limb), Trophic factors (TF)	GDNF modulates sweat pad innervation	**YES**, Tg GDNF receptor, RET mRNA increased
					Lumbar spinal cord, Sweat input to hind limb	Spinal cord shows aSyn pathology	**YES**, Mitoxy reduced Tg Veh Synucleinopathy
3NP ± Mitoxy Exp	**Vehicle alone**	**3NP alone**	**3NP +Mitoxy**	**Mitoxy alone**			**Did Mitoxy protect WT, Tg?**
Rotarod **WT**	Normal **WT** Baseline	Impaired	Impaired, but < 3NP alone	= **WT** Baseline	Cerebellum (Cb)	Cb controls balance & coordination, 3NP is toxic	**YES**, Mitoxy blocks tox & improved rotarod
Rotarod **Tg**	Impaired **Tg** Baseline	Impaired	Same as **Tg** Baseline	> **Tg** Baseline = **WT** Baseline	Cerebellum (Cb)	Cb controls balance & coordination, 3NP is toxic	**YES**, Mitoxy blocks tox & improved rotarod
SDH Activity **WT**	**WT** Baseline	Impaired	Similar to **WT** Baseline	≥ **WT** Baseline	Cerebellar mitochondria	3NP inhibits SDH activity	**YES**, Mitoxy improves SDH activity
SDH Activity **Tg**	**Tg** Baseline	Impaired	Similar to **Tg** Baseline	≥ **WT** or **Tg** Baseline	Cerebellar mitochondria	3NP inhibits SDH activity	**YES**, Mitoxy improves SDH activity

Legend: Abnormal (Abn), Cerebellum (Cb), Cortex (Cx), Corpus Callosum (CC), Experiment (Exp), Mitoxy (FTY720-Mitoxy), Succinate Dehydrogenase (SDH), Toxicity (tox), Trophic factor (TF), Transgenic (Tg), Vehicle (Veh), Wild type (WT), with (w/), #Cerebellum microglial activation